LUPUS SCIENCE & MEDICINE™

Glomerular mTORC1 activation was associated with podocytes to endothelial cells communication in lupus nephritis

Xiaotian Liu ,[1,2,3,4,5] Zhaomin Mao ,[1,2,3,4,5] Mo Yuan ,[1,2,3,4,5] Linlin Li,[1,2,3,4,5] Ying Tan,[1,2,3,4,5] Zhen Qu,[6] Min Chen,[1,2,3,4,5] Feng Yu [6]

To cite: Liu X, Mao Z, Yuan M, *et al*. Glomerular mTORC1 activation was associated with podocytes to endothelial cells communication in lupus nephritis. *Lupus Science & Medicine* 2023;**10**:e000896. doi:10.1136/lupus-2023-000896

► Additional supplemental material is published online only. To view, please visit the journal online (http://dx.doi.org/10.1136/lupus-2023-000896).

XL, ZM and MY contributed equally.

Received 4 January 2023
Accepted 15 April 2023

For numbered affiliations see end of article.

Correspondence to
Dr Ying Tan; tanying@bjmu.edu.cn and Dr Zhen Qu; janequ82@sina.com

ABSTRACT

Objective This study was initiated to evaluate the mammalian target of the rapamycin (mTOR) signalling pathway involved in renal endothelial-podocyte crosstalk in patients with lupus nephritis (LN).

Methods We compared the kidney protein expression patterns of 10 patients with LN with severe endothelial-podocyte injury and 3 patients with non-severe endothelial-podocyte injury on formalin-fixed paraffin-embedded kidney tissues using label-free liquid chromatography-mass spectrometry for quantitative proteomics analysis. Podocyte injury was graded by foot process width (FPW). The severe group was referred to patients with both glomerular endocapillary hypercellularity and FPW >1240 nm. The non-severe group included patients with normal endothelial capillaries and FPW in the range of 619~1240 nm. Gene Ontology (GO) enrichment analyses were performed based on the protein intensity levels of differentially expressed proteins in each patient. An enriched mTOR pathway was selected, and the activation of mTOR complexes in renal biopsied specimens was further verified in 176 patients with LN.

Results Compared with those of the non-severe group, 230 proteins were upregulated and 54 proteins were downregulated in the severe group. Furthermore, GO enrichment analysis showed enrichment in the 'positive regulation of mTOR signalling' pathway. The glomerular activation of mTOR complex 1 (mTORC1) was significantly increased in the severe group compared with the non-severe group (p=0.034), and mTORC1 was located in podocytes and glomerular endothelial cells. Glomerular activation of mTORC1 was positively correlated with endocapillary hypercellularity (r=0.289, p<0.001) and significantly increased in patients with both endocapillary hypercellularity and FPW >1240 nm (p<0.001).

Conclusions Glomerular mTORC1 was highly activated in patients with both glomerular endocapillary hypercellularity and podocyte injury, which might be involved in podocytes to endothelial cells communication in lupus nephritis.

WHAT IS ALREADY KNOWN ON THIS TOPIC

⇒ Endothelial cell-podocyte crosstalk might play a critical role in glomerular injury in lupus nephritis, and its regulatory molecular mechanisms still need to be explored.

WHAT THIS STUDY ADDS

⇒ Glomerular mammalian target of the rapamycin (mTOR) complex 1 activation might be involved in podocytes to endothelial cells communication in lupus nephritis.

HOW THIS STUDY MIGHT AFFECT RESEARCH, PRACTICE OR POLICY

⇒ Rational inhibition of mTOR after evaluating the renal activation of mTOR may especially help rescue glomerular injury.

INTRODUCTION

SLE is a chronic autoimmune disease that affects multiple organs, and the kidneys are involved in nearly 60% of patients.[1 2] Glomeruli are the main target of inflammation and immune deposits in lupus nephritis (LN).[2 3] Both the 2018 International Society of Nephrology/Renal Pathology Society (ISN/RPS) classification for LN and National Institutes of Health (NIH) activity and chronicity indices highlighted the clinical value of glomerular lesions in LN.[3]

Our previous studies suggested that glomerular endothelial cells and podocyte injury were both prominent lesions in LN.[4–7] In particular, the loss of podocyte integrity measured by foot process width (FPW) was positively correlated with the level of proteinuria, and a threshold FPW >1240 nm was identified to differentiate nephrotic proteinuria from non-nephrotic proteinuria in LN.[6] More importantly, the renal pathological scores of endothelial cell swelling and/or proliferation were positively correlated with FPW in patients with LN complicated with thrombotic microangiopathy (TMA).[7] The vascular endothelial growth factor (VEGF) and endothelin-1 system between glomerular endothelial cells and podocytes might play a critical role in the association between endothelial and podocyte injury,[7–11] although a more precise molecular signalling pathway concerning their crosstalk remains to be further elucidated.

Mammalian target of rapamycin (mTOR) is an evolutionarily conserved serine-threonine kinase that regulates cell growth, proliferation, metabolism and survival in response to hormonal and nutrient signals.[12–15] Increasing evidence indicates that mTOR plays an important role in the regulation of renal cell homeostasis and autophagy.[14–16] More interestingly, our previous work showed that high glomerular activation of mTOR complex 1 and 2 (mTORC1/2) was observed in endothelial cells and podocytes in patients with LN.[17] The activation of glomerular mTORC1 was especially associated with pathological endocapillary hypercellularity and clinical proteinuria.[17] Thus, we propose that mTOR signalling pathways may be involved in the endothelial-podocyte crosstalk in LN.

Here, we initially evaluated the alterations in protein expression profiles based on proteomics in the renal specimens of patients with LN with different degrees of endothelial cell and podocyte injury, and intended to uncover the role of mTOR signalling pathways in the endothelial-podocyte crosstalk of the disease with larger samples.

MATERIALS AND METHODS

Patients

Complete clinical and pathological data from 13 patients with renal biopsy-proven LN for proteomic analysis (the baseline data are listed in online supplemental table 1) and 176 patients with renal biopsy-proven LN for further verified analysis (their baseline data are listed in online supplemental table 2) at Peking University First Hospital from 2003 to 2018 were collected. Among the 176 patients, 75 in the severe endothelial-podocyte group and 10 in the non-severe endothelial-podocyte group were selected for validation of the proteomic results (figure 1). To investigate the specificity of our findings, we selected 17 patients with IgA nephropathy (IgAN) as a control group: 10 patients who had endocapillary proliferation (according to the 2016 Oxford Classification of IgA nephropathy[18]) and 7 patients without endocapillary proliferation.

Clinical evaluation

The clinical data of patients with LN were extracted from the electronic medical records of Peking University First Hospital. The disease activity was assessed by the SLE Disease Activity Index (SLEDAI).[19 20] Serum ANAs and anti-double-stranded DNA antibodies were detected using an indirect commercial immunofluorescence assay. Serum C3 was determined using a rate nephelometry assay (Beckman-Coulter, IMMAGE, Fullerton, California, USA).

Renal histopathology

Renal biopsy specimens were examined according to the 2018 ISN/RPS classification system[3] by light microscopy, direct immunofluorescence and electron microscopy. Pathological parameters, including activity indices (AI)

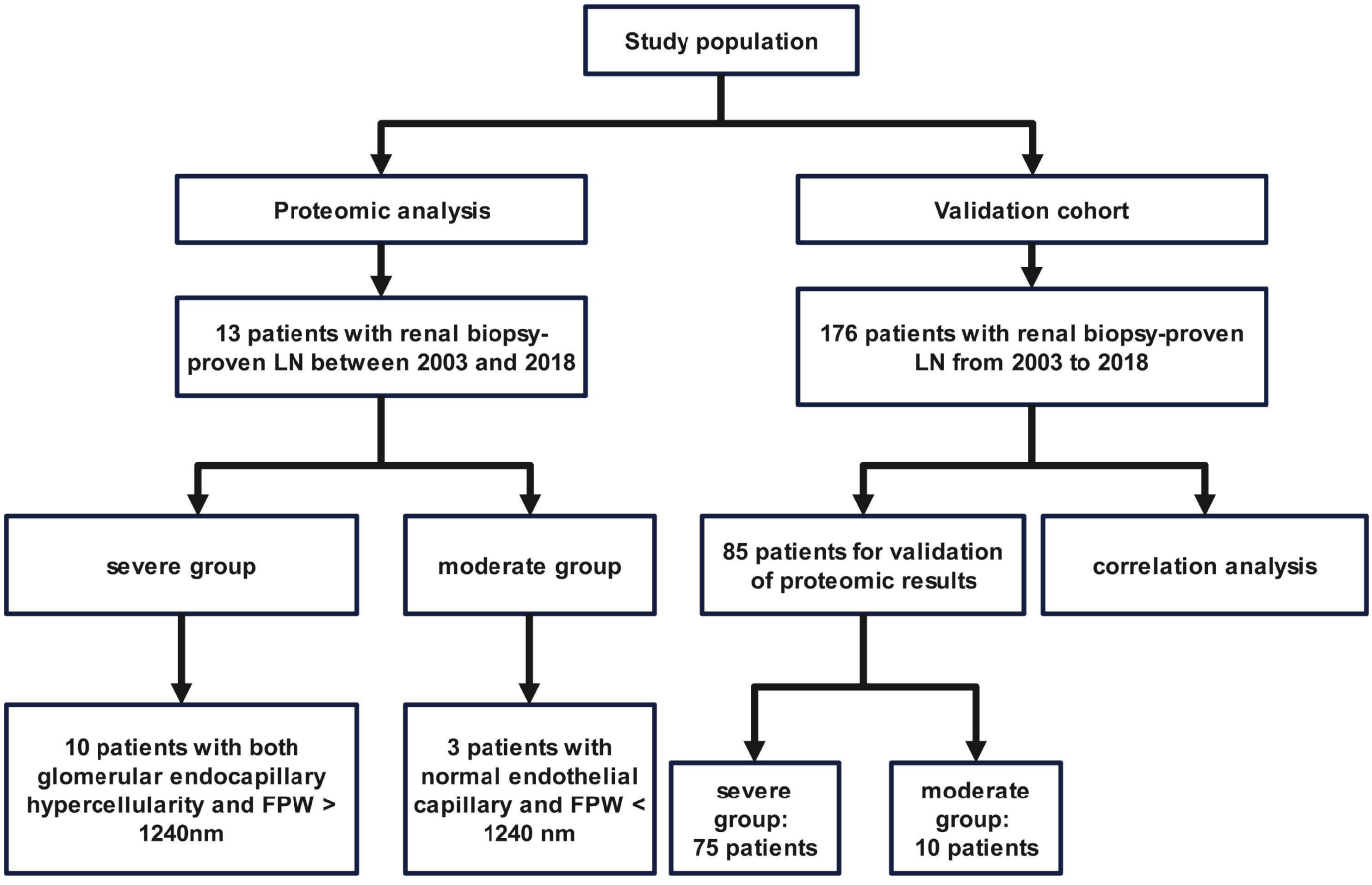

Figure 1 Flow chart of the enrolled population. FPW, foot process width; LN, lupus nephritis.

and chronicity indices (CI), were determined by semi-quantitative scoring of specific biopsy features.[3] The semi-quantification of glomerular endothelial cell injury was referred to as endocapillary hypercellularity defined by pathologists based on the NIH system.[3]

Morphometric analysis of FPW

Morphometric analysis of FPW was performed as described previously.[6 7] From each patient, the arithmetic mean of the FPW was calculated as follows:

$$FPW = \frac{\pi}{4} \times \frac{\sum GBM \quad length}{\sum foot \quad process}$$

Podocyte injury was graded by FPW, and FPW >1240 nm was the most applicable cut-off value that could differentiate nephrotic proteinuria from non-nephrotic proteinuria with a sensitivity of 81.5% and a specificity of 62.7% by ROC curve analysis in patients with LN according to our previous data.[6 7] In our centre, the normal range of FPW was 553±34 nm.[6] The bilateral reference range of normal distribution data was usually the 95% central of normal results, which was calculated as '$\bar{X} \pm 1.96S$' ($\bar{X}$ = 553, S = 34); thus, the reference range of FPW in healthy people was 486~619 nm. Severe podocyte injury was defined as an FPW >1240 nm, and the non-severe group was defined based on an FPW in the range of 619~1240 nm.

Mass spectrometry and proteomics

Formalin-fixed paraffin-embedded kidney tissues from patients with LN were digested by LysC and trypsin. After quantification of peptide concentration by Pierce Quantitative Colorimetric Peptide Assay kits, samples (2 mg each) were loaded for MS analysis. Next, label-free liquid chromatography-mass spectrometry analysis was performed on an Easy-nLC System (Thermo Fisher Scientific), and samples were analysed with a Q Exactive mass spectrometer (Thermo Fisher Scientific). The detailed mass spectrometry procedures were described in a previous study.[17 21] Raw data were searched against the UniProt Homo species database. Proteins that met the inclusion criteria had at least a twofold change, and p<0.05 was used to identify differentially expressed proteins (DEPs). GO (Gene Ontology) enrichment analyses were performed on the David website (https://david.ncifcrf.gov/).

Renal immunohistochemistry assay

Tissue samples were dewaxed and rehydrated. After antigen heated retrieval and blocking with 3% bovine serum albumin (BSA), tissues were incubated with primary rabbit antiphospho-S6 ribosomal protein (Ser 235/236) antibody or p-AKT (Ser473) (Cell Signaling Technology, Massachusetts, USA) (representative activation marker of mTORC1 and mTORC2, respectively)[17 22] or anti-CD8 (Abcam) or anti-FOXP3 antibody (Sigma), followed by incubation with secondary antibody (ZSGB-Bio, PV9001) and colouration with 3,3-diaminobenzidine. For blank controls, primary antibodies were replaced by phosphate-buffered saline (PBS). Pararenal carcinoma tissue was collected as the negative control. Cell nuclei were stained with H&E. Image-Pro Plus analysis software (V.6.0; Media Cybernetics, Dallas, Texas, USA) was used to measure the mean optical density (integrated option density/area) in renal glomeruli and tubular interstitium.

Renal immunofluorescence staining

Fresh frozen sections were blocked with 3% BSA, and then, rabbit antiphospho-S6 ribosomal protein (Ser 235/236) antibody (Cell Signaling Technology), combined with mouse antihuman CD31 (Santa Cruz) or goat antihuman synaptopodin (Santa Cruz), rabbit antihuman CD3 (Abcam) combined with mouse antihuman CD4 and CD8 (Abcam) and interleukin (IL)-17A conjugated with PE (BD Biosciences) were added and incubated overnight at 4°C, followed by the secondary antibodies Alexa Fluor 488-labelled donkey antirabbit IgG, Alexa Fluor 647-labelled donkey antimouse IgG (Abcam) or TRITC-labelled donkey antigoat IgG (Invitrogen) for 30 min at 37°C. Nuclei were stained with 4′,6-diamidino-2-phenylindole (ZSGB-Bio). For negative controls, primary antibodies were replaced by PBS. Fluorescence images were acquired with fluorescence microscopy (DM2500; Leica, Germany).

Statistical analysis

Statistical software SPSS V.25.0 (SPSS, Chicago, Illinois, USA) and Prism V.9.0 software (GraphPad, San Diego, California, USA) were used for statistical analysis. The data are presented as the mean±SD for normally distributed data or median (IQR) for non-normally distributed data, and categorical data are expressed as numbers and ratios. Differences between groups of normally distributed data were assessed using t-tests, and non-normally distributed data were assessed using non-parametric tests. Reliability analysis was carried out to test the intraclass correlation coefficient between two observers. P values <0.05 were considered statistically significant.

RESULTS

Differential proteome analysis of renal samples from patients with LN

The 13 patients with LN were divided into two groups based on the degree of endothelial cell and podocyte injuries: the severe group (10 patients with both glomerular endocapillary hypercellularity and FPW >1240 nm) and the non-severe group (3 patients with normal endothelial capillaries and FPW <1240 nm). In total, 4700 credible proteins were detected by label-free quantitative proteomic analysis, with twofold change and p≤0.05 as the differential screening conditions. Finally, 284 DEPs were selected between the severe and non-severe groups. Data are shown in online supplemental table 3. The volcano diagram suggested that 230 proteins were upregulated and 54 proteins were downregulated in the severe group compared with the non-severe group (figure 2A). The heatmaps obtained from the analysis demonstrated

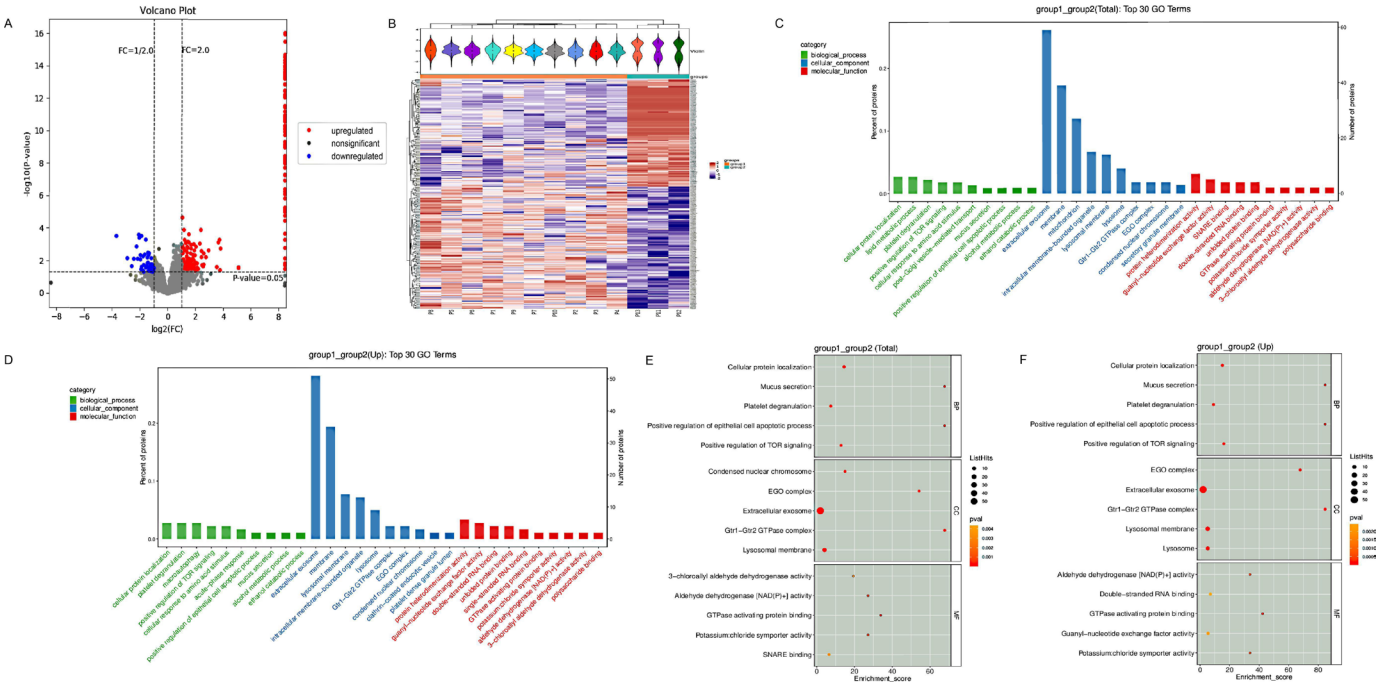

Figure 2 Quantitative proteomic and bioinformatic analyses of the renal specimens of patients with LN with severe and non-severe groups. (A) The volcano map depicts DEPs between the two groups. Red dots: upregulated proteins; green dots: downregulated proteins; grey dots: nonsignificant dots. (B) The heat maps demonstrated a clear difference in protein abundance levels across the two groups. Red bars: upregulated proteins; blue bars: downregulated proteins; green bars: sample P1-P10, non-severe group; yellow bars: sample P11-P13, severe group. (C) GO analysis items among total DEPs proteins. Green bars: biological process; blue bars: cellular complements; red bars: molecular function. (D) GO analysis items among upregulated DEPs proteins. Green bars: biological process; blue bars: cellular complements; red bars: molecular function. (E) The top five GO analysis items among total DEPs proteins. (F) The top five GO analysis items among total DEPs proteins. Group 1: severe group; group 2: non-severe group. BP, biological processes; CC, cellular components; DEP, differentially expressed protein; GO, Gene Ontology; LN, lupus nephritis; MF, molecular functions.

a clear difference in protein abundance levels across the two groups (figure 2B).

GO enrichment analysis

GO analysis was performed to enrich and cluster the DEPs of the severe group and non-severe group. Detailed information on the molecular functions, cellular components and biological processes is shown in figure 2C–D. GO annotation analysis revealed that the DEPs of the two groups were primarily involved in biological processes, including 'cellular protein localisation' (p<0.001), 'platelet degranulation' (p<0.001), 'mucus secretion' (p<0.001), 'positive regulation of mTOR signalling' (p<0.001) and 'positive regulation of epithelial cell apoptotic process' (p<0.001) (figure 2E–F). More interestingly, Ras-related GTPase (RRAG) A, RRAGB, RRAGC and RRAGD identified in the most prominently enriched pathway, 'cellular protein localisation' in GO enrichment analysis, were also covered in the biological process of 'positive regulation of mTOR signalling' (online supplemental table 4). RRAGs were demonstrated to necessarily recruit the mTOR complex to lysosomes to regulate cell growth and proliferation in response to hormonal and nutrient signals.[12 23] Thus, the positive regulation of mTOR signalling might be associated with endothelial and podocyte injuries in LN.

Validation of proteomic analysis in renal biopsied specimens of patients with LN

As mTOR signalling was found to be the most attractive pathway based on the above proteomic analysis, 85 patients with LN, 75 in the severe group and 10 in the non-severe group were selected for further validation.

Patients in the severe group presented with higher SLEDAI (p=0.049), proteinuria amount (p<0.001), serum creatinine value (p=0.010), pathological AI score (p<0.001) and CI score (p=0.043) than those in the non-severe group (table 1).

Glomerular mTORC1 activation was significantly higher in the severe group than in the non-severe group (p=0.034; figure 3A and E), and the difference was not significant in the tubulointerstitial area (p=0.129; figure 3B and E). There was no difference in mTORC2 activation between the two groups (glomeruli: p=0.643, tubulointerstitium: p=0.220, figure 3C–E). Furthermore, we found that mTORC1 staining was well colocalised with glomerular endothelial cells and podocytes in patients with LN (figure 3F).

Correlation analysis of glomerular mTORC1 activation with endothelial-podocyte involvement in patients with LN

The correlations between mTORC1 activation and endothelial-podocyte involvement were further explored in 176 patients with LN. Among them, endocapillary hypercellularity was significantly positively correlated

Table 1 Comparison of clinicopathological data between patients with LN in severe and non-severe group

	Severe (n=75)	Non-severe (n=10)	P value
Gender (male/female)	62/75	10/0	0.348
Age (years)	31 (25–40)	28 (25–38)	0.623
Proteinuria amount (g/24 hours)	3.98 (2.08–5.86)	1.64 (0.36–2.44)	<0.001
Serum creatinine (μmol/L)	98 (70–133)	59 (54–72)	0.010
C3 (mg/mL) (mean±SD)	0.41±0.20	0.51±0.18	0.145
Number of positive ANA (%)	72 (96.0)	10 (100)	0.520
Number of positive anti-dsDNA antibodies (%)	58 (77.3)	9 (90.0)	0.357
SLEDAI (mean±SD)	19±5	15±7	0.049
Renal SLEDAI (mean±SD)	11±2	8±4	0.014
Non-renal SLEDAI (mean±SD)	8±5	7±5	0.357
mTOR inhibitors treatment	0	0	NA
Renal histopathology			
Classification			0.001
Class II (%)	0 (0.0)	1 (10.0)	
Class III (%)	9 (12.0)	5 (50.0)	
Class IV (%)	61 (81.3)	2 (20.0)	
Class V (%)	5 (6.7)	2 (20.0)	
Activity index (median; IQR)	8 (6–11)	3 (2–7)	<0.001
Activity index without endocapillary hypercellularity (median; IQR)	7 (4–10)	3 (1–7)	0.001
Cellular/Fibrocellular crescents (median; IQR)	1 (0–2)	0 (0–1)	0.011
Neutrophils/Karyorrhexis (median; IQR)	1 (1–1)	0 (0–0)	<0.001
Fibrinoid necrosis (median; IQR)	0 (0–0)	0 (0–0)	0.403
Hyaline deposits (median; IQR)	1 (0–1)	0 (0–0)	<0.001
Interstitial inflammation (median; IQR)	1 (1–1)	1 (1–1)	0.154
Chronicity index score (median; IQR)	2 (1–4)	1 (0–2)	0.043
Glomerulosclerosis score (median; IQR)	0 (0–1)	0 (0–1)	0.777
Fibrous crescents (median; IQR)	0 (0–0)	0 (0–0.25)	0.853
Tubular atrophy (median; IQR)	1 (1–1)	1 (0.75–1)	0.144
Interstitial fibrosis (median; IQR)	1 (1–1)	1 (1–1)	0.335

Serum creatinine in mg/dL to mol/L, ×88.4.
dsDNA, double stranded DNA; LN, lupus nephritis; mTOR, mammalian target of the rapamycin; NA, not applicable; SLEDAI, SLE Disease Activity Index.

with mTORC1 activation (r=0.289, p<0.001), although no significant correlation was found between FPW and mTORC1 activation. Moreover, FPW was positively correlated with endocapillary hypercellularity (r=0.234, p=0.002). Patients with LN with more severe endocapillary hypercellularity presented with higher FPW (1415±312 vs 1964±1217, p=0.002) and higher glomerular activation of mTORC1 (p<0.001, figure 4A) than those without it. In particular, in patients with an FPW >1240 nm, the glomerular activation of mTORC1 was significantly higher in patients with endocapillary hypercellularity (p<0.001, figure 4A). No difference was found in glomerular activation of mTORC1 between the groups with FPW >1240 nm and FPW <1240 nm (p=0.094, figure 4B), and there was no association between FPW and mTORC1 activation (r=0.037, p=0.625). We further used the quartiles to divide the FPW into four groups, and mTORC1 activation was significantly higher in the group with FPW at 3/4 than in the group with FPW at 2/4 (p=0.042, online supplemental figure 1).

However, mTORC1 activation in glomerular and tubulointerstitial areas was similar in patients with IgAN with endothelial proliferation and those without endothelial proliferation (p=0.236, online supplemental figure 2A and p=0.379, online supplemental figure 2A–C), although mTORC1 was lightly colocalised with glomerular podocytes and endothelial cells in patients with IgAN (online supplemental figure 2D–E).

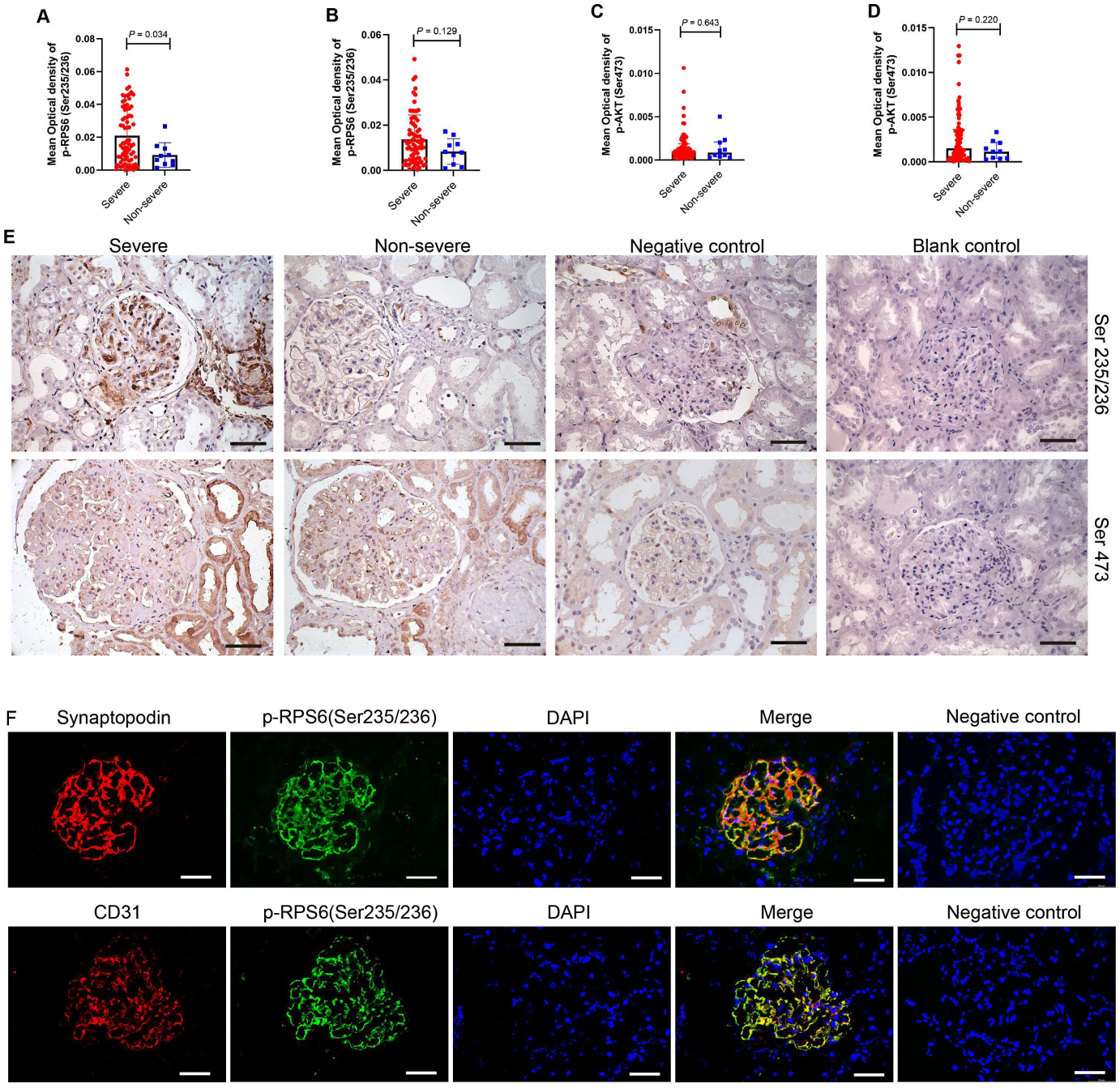

Figure 3 The expression of mTOR complex in kidneys of patients with LN between the non-severe and severe groups. The mean optical density of p-RPS6 (ser235/236) (A-B) and p-AKT (Ser473) (C-D) in the glomeruli and tubulointerstitium between severe and non-severe groups (endocapillary hypercellularity), respectively. (E) Immunohistochemical staining of p-RPS6 (ser235/236) and p-AKT (Ser473) in the glomeruli and tubulointerstitium between severe and non-severe groups, respectively. (F) Colocalisation of p-RPS6 (ser235/236) (green) and synaptopodin (green) (a marker of podocyte), CD31 (red) (a marker of endothelial cells). DAPI, 4′,6-diamidino-2-phenylindole (blue) (a marker of the nucleus); LN, lupus nephritis; mTOR, mammalian target of the rapamycin. Scale bar: 50 µm.

We further investigated the renal distribution of the T-cell subsets in patients with LN. $CD8^+$ T cells (p=0.0046, online supplemental figure 3A and E), $CD4^-CD8^-$ double-negative T cells (p=0.0052, online supplemental figures 3C, G, H) and T helper (Th)17 cells (p=0.0415, online supplemental figure 3D, I) were significantly higher in the high mTORC1 activation group. The mean optical density of regulatory T (Tregs) cells was similar between the high and low mTORC1 activation groups (p=0.3830, online supplemental figure 3B and F).

DISCUSSION/CONCLUSION

The critical role of endothelial-podocyte crosstalk in the development of glomerular lesions through the paracrine process was highlighted in some kidney diseases,

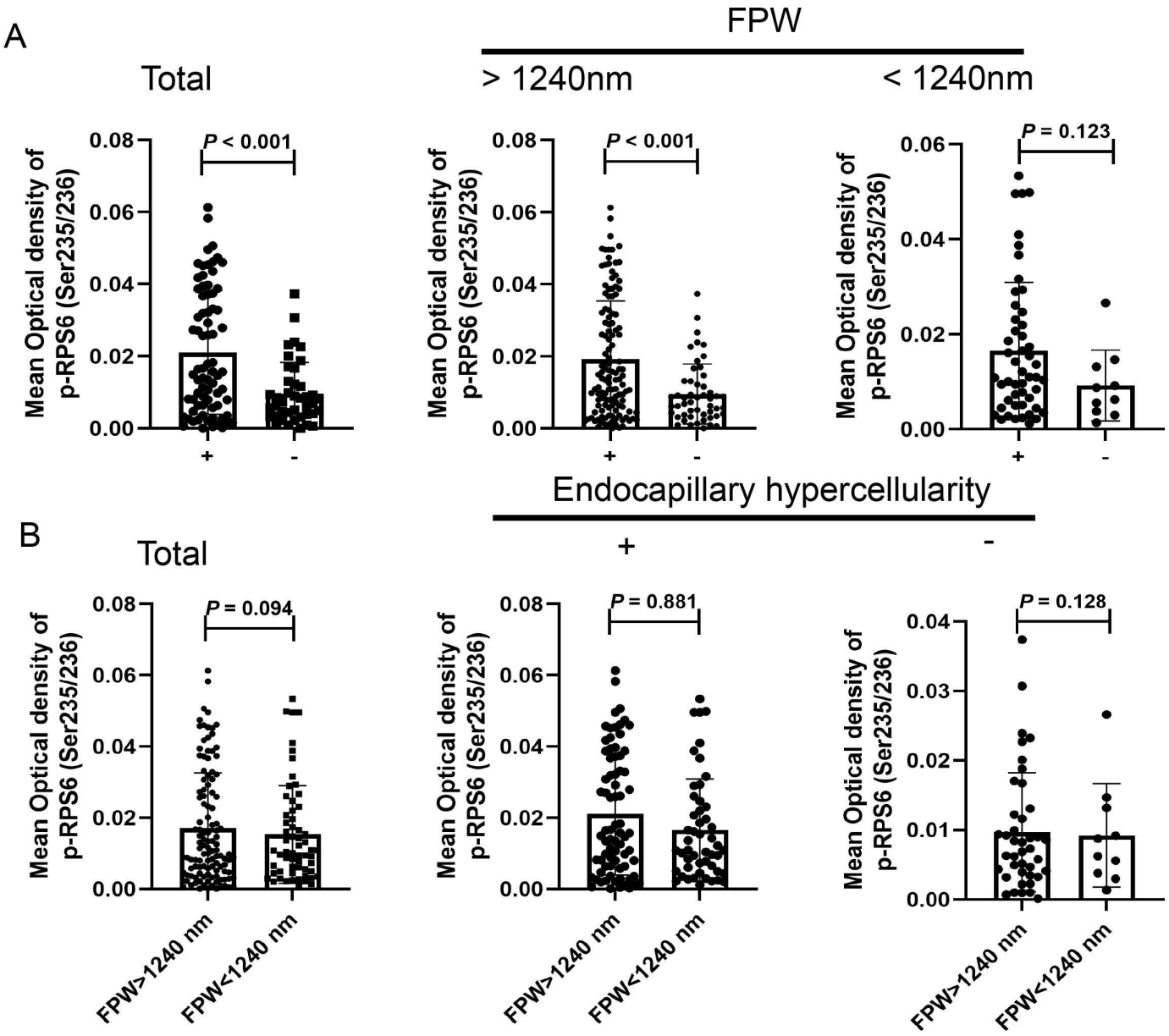

Figure 4 The association of glomerular mTORC1 activation with endocapillary hypercellularity and foot process infusion in patients with LN. (A) Mean optical density of mTORC1 in glomeruli with endocapillary hypercellularity. (B) Mean optical density of mTORC1 in glomeruli with FPW >1240 nm. '+' refers to those patients with endocapillary hypercellularity; '–' refers to those patients without endocapillary hypercellularity. FPW, foot process width; LN, lupus nephritis; mTOR, mammalian target of the rapamycin; mTORC1, mTOR complex 1.

including LN.[8–11] In the current study, we initially explored the mTOR signalling pathway associated with endocapillary hypercellularity and foot process fusion through renal proteomics analysis and verified the significant association of mTORC1 from podocytes to endothelial cells communication based on a well-defined LN cohort.

First, MS-based renal proteomics was applied to discover the difference in signalling pathways between the 'severe' endothelial cell and podocyte injury group and the 'non-severe' group. GO enrichment analysis revealed that the DEPs of the two groups were primarily involved in some biological processes, including the 'positive regulation of mTOR signalling' pathway. Moreover, 'Ras-related GTPase' DEPs were both covered in 'the positive regulation of TOR signalling' and 'cellular protein localisation' of biological process sections. Compelling evidence suggests that the Rag heterodimer (RagA/B and RagC/D) plays a critical role in amino acid signalling to mTORC1 activation by recruiting mTORC1 to the lysosomal membrane,[23] which could highlight the status of the mTORC1 pathway involved in endothelial cell and podocyte injuries in LN.

Next, our immunohistochemistry work showed that the glomerular activation of mTORC1 was associated with more severe endothelial cell and podocyte injury based on a larger sample. More importantly, mTORC1 staining was found to be well colocalised with glomerular endothelial cells and podocytes, which was consistent with

our previous work.[17] However, no significant associations were found between endothelial proliferation and the activation of mTORC1 in patients with IgAN. Thus, the mechanism of endothelial injury in IgAN and LN might be different.

Last, the correlation analysis from all 176 patients with LN suggested that the patients with more severe endocapillary hypercellularity scores presented with higher FPW and higher glomerular activation of mTORC1. Thus, we proposed that mTORC1 activation might be associated with podocyte-to-endothelial cell communication in LN.

The pathomechanism between mTORC1 activation and endothelial cell-podocyte injury remains unclear. The VEGF-endothelin-1 system has been previously confirmed as a vital process in endothelial-podocyte crosstalk in LN.[7 8 24] The activation of mTORC1 in podocytes was accompanied by increased VEGF expression in renal tissues in active patients with LN, as well as amplified activation of the mTOR signalling pathway and proliferation of endothelial cells by VEGF stimulation.[25–29] Nevertheless, the glomerular expression of VEGF was significantly decreased in patients with LN with both TMA changes and FPW ≥1240 nm in our previous results.[7] The disruption of podocytes by excess activation of mTORC1 may result in decreased VEGF, which further exacerbates endotheliosis.[30 31] Therefore, mTORC1 activation might be an upstream regulatory signal of podocyte-to-endothelial cell communication, which promotes the development of glomerular lesions in LN. More importantly, our previous study found that glomerular mTORC1 activation was strongly correlated with deteriorative clinicopathological characteristics in patients with LN.[17] It was proposed that mTOR could develop as a driver of vascular endothelial proliferation and immune activation,[13–16 22] and excessive activation of mTORC1 in podocytes might result in podocyte loss and subsequent global glomerular sclerosis in mouse models.[32 33]

Moreover, our results indicated that mTOR activation was accompanied by an expansion of T-cell populations, especially diabetes nephropathy (DN) T cells. Previous studies showed that mTORC1 activation in SLE drove the expansion of DN T cells, Th1 cells and Th17 cells and inhibited T-cell lineage specification to Tregs.[34] DN T cells promote B-cell assistance, leading to the production of pathogenic IgG and the pro-inflammatory cytokines IL-4, IL-17 and interferon-γ,[35] which might be associated with the increased autoantibody formation involved in glomerular lesions in LN. Therefore, we speculated that the activation of mTOR in T cells played a critical role in the pathogenesis of LN, which needs further exploration.

More interestingly, mTOR inhibition with sirolimus or everolimus could reduce proteinuria and improve kidney function in patients with SLE.[36–38] Inhibition of mTOR by rapamycin involved mTOR blockade in kidney native cells, reduced necrosis within T cells and DN T cells and expanded Treg populations.[39] Rational inhibition of mTOR after evaluating the renal activation of mTOR may especially help rescue glomerular endothelial and podocyte injury, which is a potential therapeutic option for LN and deserves further exploration.

Our study had some limitations. Our present study was a retrospective study based on selected phenotypes and a limited evaluation index of podocyte and endothelial cell injury. The proteomics results need to be more widely verified. T-cell activation in the renal tissues was not fully considered in our study, and the comparison with other immune-mediated glomerulonephritis needs to be verified in a larger sample size. The precise role of mTORC1 in endothelial-podocyte crosstalk remains to be further clarified.

In conclusion, glomerular mTORC1 was highly activated in patients with LN with both endocapillary hypercellularity and podocyte injuries, which might be involved in podocytes to endothelial cells communication in LN.

Author affiliations
[1]Renal Division, Peking University First Hospital, Beijing, China
[2]Institute of Nephrology, Peking University, Beijing, China
[3]Key Laboratory of Renal Disease, Ministry of Health of China, Beijing, China
[4]Key Laboratory of CKD Prevention and Treatment, Ministry of Education of China, Beijing, China
[5]Research Units of Diagnosis and Treatment of Immune-Mediated Kidney Diseases, Chinese Academy of Medical Sciences, Beijing, China
[6]Department of Nephrology, Peking University International Hospital, Beijing, China

Correction notice This article has been corrected since it was published. Co-corresponding author and equal contribution statement has been added.

Contributors XL performed the experiments, analysed the statistics and drafted the manuscript. MY and ZM performed the experiments. LL conducted the proteomic assay. FY, ZQ and MC provided intellectual content of importance to this work and revised the manuscript. YT is the guarantor and had full access to all the data and provided final approval of the submitted manuscript.

Funding This work was supported by grants from Peking University Clinical Scientist Training Program supported by "the Fundamental Research Funds for the Central Universities", the CAMS Innovation Fund for Medical Sciences (2019-I2M-5-046), Peking University International Hospital Research Grant (No. YN2020ZD03)

Competing interests None declared.

Patient and public involvement Patients and/or the public were not involved in the design, or conduct, or reporting, or dissemination plans of this research.

Patient consent for publication Not applicable.

Ethics approval This study was approved by Ethics Committee of Peking University First Hospital (2017 (1333)). Participants gave informed consent to participate in the study before taking part.

Provenance and peer review Not commissioned; externally peer reviewed.

Data availability statement Data are available in a public, open access repository.

ORCID iDs
Xiaotian Liu http://orcid.org/0000-0002-0142-0782
Zhaomin Mao http://orcid.org/0000-0002-9029-7252
Mo Yuan http://orcid.org/0000-0001-5372-0106
Feng Yu http://orcid.org/0000-0003-3060-6233

REFERENCES

1 Anders H-J, Saxena R, Zhao M-H, *et al*. Lupus nephritis. *Nat Rev Dis Primers* 2020;6:7.
2 Yu F, Haas M, Glassock R, *et al*. Redefining lupus nephritis: clinical implications of pathophysiologic subtypes. *Nat Rev Nephrol* 2017;13:483–95.
3 Bajema IM, Wilhelmus S, Alpers CE, *et al*. Revision of the International Society of nephrology/renal pathology Society classification for lupus nephritis: clarification of definitions, and modified National Institutes of health activity and chronicity indices. *Kidney Int* 2018;93:789–96.
4 Wu L-H, Yu F, Tan Y, *et al*. Inclusion of renal vascular lesions in the 2003 ISN/RPS system for classifying lupus nephritis improves renal outcome predictions [J]. *Kidney International* 2013;83:715–23.
5 Song D, Wu L, Wang F, *et al*. The spectrum of renal thrombotic microangiopathy in lupus nephritis. *Arthritis Res Ther* 2013;15:R12.
6 Wang Y, Yu F, Song D, *et al*. Podocyte involvement in lupus nephritis based on the 2003 ISN/RPS system: a large cohort study from a single centre. *Rheumatology (Oxford)* 2014;53:1235–44.
7 Yuan M, Tan Y, Wang Y, *et al*. The associations of endothelial and podocyte injury in proliferative lupus nephritis: from observational analysis to in vitro study. *Lupus* 2019;28:347–58.
8 Ebefors K, Wiener RJ, Yu L, *et al*. Endothelin receptor-A mediates degradation of the glomerular endothelial surface layer via pathologic crosstalk between activated podocytes and glomerular endothelial cells. *Kidney Int* 2019;96:957–70.
9 van de Lest NA, Bakker AE, Dijkstra KL, *et al*. Endothelial endothelin receptor A expression is associated with podocyte injury and oxidative stress in patients with focal segmental glomerulosclerosis. *Kidney Int Rep* 2021;6:1939–48.
10 Daehn I, Casalena G, Zhang T, *et al*. Endothelial mitochondrial oxidative stress determines podocyte depletion in segmental glomerulosclerosis. *J Clin Invest* 2014;124:1608–21.
11 van Aanhold CCL, Bos M, Mirabito Colafella KM, *et al*. n.d. Thrombomodulin is upregulated in the kidneys of women with pre-eclampsia. *Sci Rep*;11.
12 Jewell JL, Russell RC, Guan K-L. Amino acid signalling upstream of mTOR. *Nat Rev Mol Cell Biol* 2013;14:133–9.
13 Weichhart T, Hengstschläger M, Linke M. Regulation of innate immune cell function by mTOR. *Nat Rev Immunol* 2015;15:599–614.
14 Lieberthal W, Levine JS. The role of the mammalian target of rapamycin (mTOR) in renal disease. *Journal of the American Society of Nephrology* 2009;20:2493–502.
15 Fantus D, Rogers NM, Grahammer F, *et al*. Roles of mTOR complexes in the kidney: implications for renal disease and transplantation. *Nat Rev Nephrol* 2016;12:587–609.
16 Guertin DA, Sabatini DM. Defining the role of mTOR in cancer. *Cancer Cell* 2007;12:9–22.
17 Mao Z, Tan Y, Tao J, *et al*. Renal mTORC1 activation is associated with disease activity and prognosis in lupus nephritis. *Rheumatology (Oxford)* 2022;61:3830–40.
18 Trimarchi H, Barratt J, Cattran DC, *et al*. Oxford classification of IgA nephropathy 2016: an update from the IgA nephropathy classification Working group. *Kidney International* 2017;91:1014–21.
19 Liang MH, Socher SA, Larson MG, *et al*. Reliability and validity of six systems for the clinical assessment of disease activity in systemic lupus erythematosus. *Arthritis Care Res* 1989;32:1107–18. 10.1002/anr.1780320909 Available: http://doi.wiley.com/10.1002/anr.v32:9
20 Bombardier C, Gladman DD, Urowitz MB, *et al*. Derivation of the SLEDAI. A disease activity index for lupus patients. The Committee on prognosis studies in SLE. *Arthritis Rheum* 1992;35:630–40.
21 Chen Y-Y, Ding Y, Li L-L, *et al*. Proteomic profiling of kidney samples in patients with pure membranous and proliferative lupus nephritis. *Lupus* 2022;31:837–47.
22 Canaud G, Bienaimé F, Tabarin F, *et al*. Inhibition of the mTORC pathway in the antiphospholipid syndrome. *N Engl J Med* 2014;371:303–12.
23 Anandapadamanaban M, Masson GR, Perisic O, *et al*. Architecture of human RAG GTPase heterodimers and their complex with mTORC1. *Science* 2019;366:203–10.
24 Avihingsanon Y, Benjachat T, Tassanarong A, *et al*. Decreased renal expression of vascular endothelial growth factor in lupus nephritis is associated with worse prognosis. *Kidney International* 2009;75:1340–8.
25 Yoshibayashi M, Kume S, Yasuda-Yamahara M, *et al*. Protective role of podocyte autophagy against glomerular endothelial dysfunction in diabetes. *Biochemical and Biophysical Research Communications* 2020;525:319–25.
26 Miaomiao W, Chunhua L, Xiaochen Z, *et al*. Autophagy is involved in regulating VEGF during high-glucose-induced podocyte injury. *Mol Biosyst* 2016;12:2202–12.
27 Avihingsanon Y, Phumesin P, Benjachat T, *et al*. Measurement of urinary chemokine and growth factor messenger RNAs: a noninvasive monitoring in lupus nephritis. *Kidney Int* 2006;69:747–53.
28 Navarro C, Candia-Zúñiga L, Silveira LH, *et al*. Vascular endothelial growth factor plasma levels in patients with systemic lupus erythematosus and primary antiphospholipid syndrome. *Lupus* 2002;11:21–4.
29 Husain A, Khadka A, Ehrlicher A, *et al*. Substrate stiffening promotes VEGF-A functions via the PI3K/Akt/mTOR pathway. *Biochem Biophys Res Commun* 2022;586:27–33.
30 Eremina V, Cui S, Gerber H, *et al*. Vascular endothelial growth factor a signaling in the podocyte-endothelial compartment is required for mesangial cell migration and survival. *Journal of the American Society of Nephrology* 2006;17:724–35.
31 Eremina V, Jefferson JA, Kowalewska J, *et al*. Vegf inhibition and renal thrombotic microangiopathy. *N Engl J Med* 2008;358:1129–36.
32 Inoki K, Mori H, Wang J, *et al*. Mtorc1 activation in podocytes is a critical step in the development of diabetic nephropathy in mice. *J Clin Invest* 2011;121:2181–96.
33 Gödel M, Hartleben B, Herbach N, *et al*. Role of mTOR in podocyte function and diabetic nephropathy in humans and mice. *J Clin Invest* 2011;121:2197–209.
34 Caza T, Wijewardena C, Al-rabadi L, *et al*. Cell type-specific mechanistic target of rapamycin-dependent distortion of autophagy pathways in lupus nephritis. *Translational Research* 2022;245:55–81.
35 Sieling PA, Porcelli SA, Duong BT, *et al*. Human double-negative T cells in systemic lupus erythematosus provide help for IgG and are restricted by CD1c. *The Journal of Immunology* 2000;165:5338–44.
36 Lai Z-W, Kelly R, Winans T, *et al*. Sirolimus in patients with clinically active systemic lupus erythematosus resistant to, or intolerant of, conventional medications: a single-arm, open-label, phase 1/2 trial. *Lancet* 2018;391:1186–96.
37 Piranavan P, Perl A. Improvement of renal and non-renal SLE outcome measures on sirolimus therapy-a 21-year follow-up study of 73 patients. *Clin Immunol* 2021;229:108781.
38 Yap DY, Ma MK, Tang CS, *et al*. Proliferation signal inhibitors in the treatment of lupus nephritis: preliminary experience. *Nephrology (Carlton)* 2012;17:676–80. 10.1111/j.1440-1797.2012.01646.x Available: http://doi.wiley.com/10.1111/nep.2012.17.issue-8
39 Battaglia M, Stabilini A, Migliavacca B, *et al*. Rapamycin promotes expansion of functional CD4+CD25+FoxP3+ regulatory T cells of both healthy subjects and type 1 diabetic patients. *J Immunol* 2006;177:8338–47.

Supplementary materials

Supplementary Table 1. The baseline data of 13 lupus nephritis patients for proteomic analysis

Patient	Group	Age/ gender	SLEDAI	Proteinuria, g/day	Scr, μ mol/l	C3, g/L	Anti-nuclear antibody	Anti-dsDNA antibody	Renal Histopathology				
									Classification	AI/CI	Endocapillary hypercellularity	Subendothelial hyaline deposits	FPW, nm
1	1	18/F	14	0.45	78.5	0.20	+	+	IV	3/0	1	1	1267
2	1	42/F	15	0.84	63.0	0.21	+	-	III	6/3	1	1	1328
3	1	69/F	26	6.21	108.9	0.27	+	+	IV	1/0	1	0	2711
4	1	21/M	16	4.35	127.9	0.23	+	+	IV	4/2	1	1	2490
5	1	38/F	16	1.81	67.0	NA	-	-	IV	1/0	1	0	1458
6	1	27/F	2	6.32	48.2	0.44	+	+	III	5/3	1	0	3752
7	1	38/F	18	5.38	133	0.22	+	+	IV	14/4	1	1	1623
8	1	26/M	18	9.30	135	0.37	+	+	IV	6/0	1	0	2379
9	1	34/M	12	0.84	81.1	0.47	+	+	III	4/0	1	1	2277
10	1	40/F	17	4.08	77.0	0.60	+	+	III	6/3	1	0	1529
11	2	13/F	12	0.16	44.0	0.57	+	+	V	0/0	0	0	1216
12	2	42/M	14	3.15	79.5	0.42	+	+	V	0/1	0	0	1172
13	2	22/F	17	9.50	45.9	0.50	-	-	V	2/1	0	1	937

Note: F: female; M: male; Scr: serum creatinine; AI: acute index; CI: chronic index; FPW: foot process width; SLEDAI, systemic lupus erythematosus disease activity index; Anti-dsDNA antibody, anti-double-stranded DNA. Group 1: severe group; group 2: Non-severe group.

Liu X, *et al. Lupus Sci Med* 2023; 10:e000896. doi: 10.1136/lupus-2023-000896

Supplementary Table 2. General data of 176 lupus nephritis patients

Index	Description
Clinical Evaluation and Laboratory Assessment	
Sex (male/female), no.	22/154
Age, (yrs), mean ± SD	33±12
SLEDAI, mean ± SD	17±6
Proteinuria (g/24 h), (median; IQR)	2.8(1.4-4.9)
Scr (μmol/L), (median; IQR)	75.6(56.1-109.5)
C3 (g/L), mean ± SD	0.4(0.3-0.6)
Anti-nuclear antibody (+)(%)	170(96.5)
Anti-double-stranded DNA antibody (+)(%)	117(66.5)
Renal Histopathology	
Classification	
Class II (%)	8(4.5)
Class III (%)	31(17.6)
Class IV (%)	100(56.8)
Class V (%)	37(21.0)
Acute index score (median; IQR)	6(3-9)
Endocapillary hypercellularity (median; IQR)	1(0-1)
Cellular/fibrocellular crescents (median; IQR)	1(0-1)
Neutrophils/karyorrhexis (median; IQR)	1(0-1)
Fibrinoid necrosis (median; IQR)	0(0-0)
Hyaline deposits (median; IQR)	0(0-1)
Interstitial Inflammation (median; IQR)	1(1-1)
Chronicity index score (median; IQR)	2(1-3)
Glomerulosclerosis score (median; IQR)	0(0-1)
Fibrous crescents (median; IQR)	0(0-0)
Tubular atrophy (median; IQR)	1(1-1)
Interstitial fibrosis (median; IQR)	1(1-1)
FPW, mean ± SD	1489(1108-2190)

SLEDAI, systemic lupus erythematosus disease activity index; Scr, serum creatinine; IQR, interquartile range; FPW, foot process width.

Supplementary Table 3. The 284 differentially expressed proteins between severe and moderate groups

UniProt ID	Description	Gene Name	P-value	Fold Change
54 differentially downregulated expressed proteins				
TTC7B	tetratricopeptide repeat domain 7B(TTC7B)	TTC7B	0.00029316	0.077312192
THEM6	thioesterase superfamily member 6(THEM6)	THEM6	0.00717857	0.131357655
GSTA1	glutathione S-transferase alpha 1(GSTA1)	GSTA1	0.02284454	0.165482199
DMD	dystrophin(DMD)	DMD	0.00778303	0.184909622
UCK1	uridine-cytidine kinase 1(UCK1)	UCK1	0.00136639	0.207814829
KRT6B	keratin 6B(KRT6B)	KRT6B	0.00755151	0.224924313
TMEM38B	transmembrane protein 38B(TMEM38B)	TMEM38B	0.00024419	0.235351148
CLRN3	clarin 3(CLRN3)	CLRN3	0.00038324	0.242921065
CTNNBL1	catenin beta like 1(CTNNBL1)	CTNNBL1	0.00851879	0.256355677
P3H1	prolyl 3-hydroxylase 1(P3H1)	P3H1	0.00455301	0.258077103
MRPS35	mitochondrial ribosomal protein S35(MRPS35)	MRPS35	0.03526684	0.261025053
OXCT1	3-oxoacid CoA-transferase 1(OXCT1)	OXCT1	0.02407023	0.268959303
PDE4DIP	phosphodiesterase 4D interacting protein(PDE4DIP)	PDE4DIP	0.00029979	0.271514012
INHBE	inhibin beta E subunit(INHBE)	INHBE	0.00556809	0.291447357
PYROXD2	pyridine nucleotide-disulphide oxidoreductase domain 2(PYROXD2)	PYROXD2	0.03936044	0.291695467
NUDT12	nudix hydrolase 12(NUDT12)	NUDT12	0.01837059	0.30104546
PARS2	prolyl-tRNA synthetase 2, mitochondrial (putative)(PARS2)	PARS2	0.04929612	0.301740162
CSTF3	cleavage stimulation factor subunit 3(CSTF3)	CSTF3	0.00407399	0.316605668
FBXO22	F-box protein 22(FBXO22)	FBXO22	0.02514262	0.330503658
GNG7	G protein subunit gamma 7(GNG7)	GNG7	0.00050299	0.33273349
SCOC	short coiled-coil protein(SCOC)	SCOC	0.02164541	0.343965189
RAD21	RAD21 cohesin complex component(RAD21)	RAD21	0.02213457	0.354702617
CLCC1	chloride channel CLIC like 1(CLCC1)	CLCC1	0.02342699	0.362421538
PPFIA1	PTPRF interacting protein alpha 1(PPFIA1)	PPFIA1	0.00659459	0.365308791
TMEM177	transmembrane protein 177(TMEM177)	TMEM177	0.01404454	0.367203637
TTYH3	tweety family member 3(TTYH3)	TTYH3	0.01286454	0.367992952
MRPL45	mitochondrial ribosomal protein L45(MRPL45)	MRPL45	0.00325620	0.371773584
AFMID	arylformamidase(AFMID)	AFMID	0.04200421	0.378176384
KIFAP3	kinesin associated protein 3(KIFAP3)	KIFAP3	0.00456015	0.387236768
SIN3A	SIN3 transcription regulator family member A(SIN3A)	SIN3A	0.00342890	0.395549978
FOXRED1	FAD dependent oxidoreductase domain containing 1(FOXRED1)	FOXRED1	0.03087931	0.399400402

Be continued

ZBTB20	zinc finger and BTB domain containing 20(ZBTB20)	ZBTB20	0.03322467	0.403870218
ENPP6	ectonucleotide pyrophosphatase/phosphodiesterase 6(ENPP6)	ENPP6	0.01736699	0.421126942
ACADL	acyl-CoA dehydrogenase, long chain(ACADL)	ACADL	0.03640342	0.424154494
RSF1	remodeling and spacing factor 1(RSF1)	RSF1	0.01952626	0.424562725
TFB1M	transcription factor B1, mitochondrial(TFB1M)	TFB1M	0.04271253	0.427427311
SPRYD4	SPRY domain containing 4(SPRYD4)	SPRYD4	0.02171357	0.428377868
MTMR6	myotubularin related protein 6(MTMR6)	MTMR6	0.00699873	0.438694964
RABL3	RAB, member of RAS oncogene family like 3(RABL3)	RABL3	0.01777239	0.441278593
MRPL28	mitochondrial ribosomal protein L28(MRPL28)	MRPL28	0.01697911	0.443145568
SF3B5	splicing factor 3b subunit 5(SF3B5)	SF3B5	0.02742457	0.443718947
POLDIP2	DNA polymerase delta interacting protein 2(POLDIP2)	POLDIP2	0.01679660	0.447543817
LRRC57	leucine rich repeat containing 57(LRRC57)	LRRC57	0.03429539	0.44867217
NUDT19	nudix hydrolase 19(NUDT19)	NUDT19	0.03731068	0.453037687
TRIM47	tripartite motif containing 47(TRIM47)	TRIM47	0.01837688	0.457032583
PTPMT1	protein tyrosine phosphatase, mitochondrial 1(PTPMT1)	PTPMT1	0.02629364	0.464633517
FGF2	fibroblast growth factor 2(FGF2)	FGF2	0.04937211	0.468396103
IRAK2	interleukin 1 receptor associated kinase 2(IRAK2)	IRAK2	0.04229640	0.471990476
PRKACG	protein kinase cAMP-activated catalytic subunit gamma(PRKACG)	PRKACG	0.04281017	0.472000112
TBRG4	transforming growth factor beta regulator 4(TBRG4)	TBRG4	0.03199141	0.473067785
CBR4	carbonyl reductase 4(CBR4)	CBR4	0.03575183	0.479705487
VAMP2	vesicle associated membrane protein 2(VAMP2)	VAMP2	0.04104667	0.4845826
CIAO2B	family with sequence similarity 96 member B(FAM96B)	CIAO2B	0.02618342	0.488470407
BCKDK	branched chain ketoacid dehydrogenase kinase(BCKDK)	BCKDK	0.02885033	0.498519952
230 differentially upregulated expressed proteins				
ALDH3B1	aldehyde dehydrogenase 3 family member B1(ALDH3B1)	ALDH3B1	0.02476132	2.002914706
ALDH3B2	aldehyde dehydrogenase 3 family member B2(ALDH3B2)	ALDH3B2	0.02476132	2.002914706
VWA5A	von Willebrand factor A domain containing	VWA5A	0.03798363	2.003600521

Be continued

	5A(VWA5A)			
DHX36	DEAH-box helicase 36(DHX36)	DHX36	0.04064060	2.004017728
ATG4B	autophagy related 4B cysteine peptidase(ATG4B)	ATG4B	0.02172533	2.009630197
HNRNPUL1	heterogeneous nuclear ribonucleoprotein U like 1(HNRNPUL1)	HNRNPUL1	0.00377826	2.009693419
PLD3	phospholipase D family member 3(PLD3)	PLD3	0.02096436	2.020558245
PFN2	profilin 2(PFN2)	PFN2	0.00919077	2.028756599
GSDMD	gasdermin D(GSDMD)	GSDMD	0.02498522	2.036853327
DYNLT1	dynein light chain Tctex-type 1(DYNLT1)	DYNLT1	0.04644383	2.039420137
APOD	apolipoprotein D(APOD)	APOD	0.02243585	2.046304926
HNRNPLL	heterogeneous nuclear ribonucleoprotein L like(HNRNPLL)	HNRNPLL	0.01263359	2.052981558
THBS1	thrombospondin 1(THBS1)	THBS1	0.00002145	2.073027491
SURF4	surfeit 4(SURF4)	SURF4	0.00164886	2.075621015
SNRPB2	small nuclear ribonucleoprotein polypeptide B2(SNRPB2)	SNRPB2	0.03194093	2.075809865
DAD1	defender against cell death 1(DAD1)	DAD1	0.01532929	2.07686187
SAR1A	secretion associated Ras related GTPase 1A(SAR1A)	SAR1A	0.00108335	2.077583213
GDA	guanine deaminase(GDA)	GDA	0.03799960	2.078854824
HKDC1	hexokinase domain containing 1(HKDC1)	HKDC1	0.01057816	2.0849862
EFHD2	EF-hand domain family member D2(EFHD2)	EFHD2	0.01543222	2.087649691
LGALS1	galectin 1(LGALS1)	LGALS1	0.00343413	2.093452504
NAA50	N(alpha)-acetyltransferase 50, NatE catalytic subunit(NAA50)	NAA50	0.02936376	2.130292774
SERPINB9	serpin family B member 9(SERPINB9)	SERPINB9	0.01628502	2.139430796
TM9SF3	transmembrane 9 superfamily member 3(TM9SF3)	TM9SF3	0.03697617	2.144075132
MAPRE3	microtubule associated protein RP/EB family member 3(MAPRE3)	MAPRE3	0.00835519	2.151476875
TMX4	thioredoxin related transmembrane protein 4(TMX4)	TMX4	0.02909259	2.184902863
SLC35B2	solute carrier family 35 member B2(SLC35B2)	SLC35B2	0.00800823	2.185486383
RCC1	regulator of chromosome condensation 1(RCC1)	RCC1	0.01954603	2.198793721
MCU	mitochondrial calcium uniporter(MCU)	MCU	0.04290235	2.204655135
TWF2	twinfilin actin binding protein 2(TWF2)	TWF2	0.04892754	2.214270152
VAV2	vav guanine nucleotide exchange factor 2(VAV2)	VAV2	0.03777287	2.234336543
RCN2	reticulocalbin 2(RCN2)	RCN2	0.00170138	2.266055216
SRP72	signal recognition particle 72(SRP72)	SRP72	0.00012557	2.269274151

Be continued

IFI30	IFI30, lysosomal thiol reductase(IFI30)	IFI30	0.03974131	2.269828935
CDC73	cell division cycle 73(CDC73)	CDC73	0.02438375	2.270544319
SRP68	signal recognition particle 68(SRP68)	SRP68	0.00049103	2.278253305
RSL1D1	ribosomal L1 domain containing 1(RSL1D1)	RSL1D1	0.04559553	2.289740863
SLC12A6	solute carrier family 12 member 6(SLC12A6)	SLC12A6	0.00229814	2.303296468
SLC12A4	solute carrier family 12 member 4(SLC12A4)	SLC12A4	0.00229814	2.303296468
DFFA	DNA fragmentation factor subunit alpha(DFFA)	DFFA	0.01257109	2.310542937
GNB4	G protein subunit beta 4(GNB4)	GNB4	0.02069002	2.310764999
CRKL	CRK like proto-oncogene, adaptor protein(CRKL)	CRKL	0.02617146	2.342853306
IGF2BP2	insulin like growth factor 2 mRNA binding protein 2(IGF2BP2)	IGF2BP2	0.01449741	2.349553885
TXLNA	taxilin alpha(TXLNA)	TXLNA	0.03192475	2.364080274
BLOC1S4	biogenesis of lysosomal organelles complex 1 subunit 4(BLOC1S4)	BLOC1S4	0.03502529	2.371418642
TGM2	transglutaminase 2(TGM2)	TGM2	0.01902131	2.378156815
IGKV1-8	immunoglobulin kappa variable 1-8(IGKV1-8)	IGKV1-8	0.01750446	2.407530225
FMNL3	formin like 3(FMNL3)	FMNL3	0.01622723	2.42061035
FMNL2	formin like 2(FMNL2)	FMNL2	0.01622723	2.42061035
ATP13A1	ATPase 13A1(ATP13A1)	ATP13A1	0.02376667	2.435083722
PI4K2A	phosphatidylinositol 4-kinase type 2 alpha(PI4K2A)	PI4K2A	0.03384578	2.445719007
COL15A1	collagen type XV alpha 1 chain(COL15A1)	COL15A1	0.01745922	2.453830888
VAMP8	vesicle associated membrane protein 8(VAMP8)	VAMP8	0.00077360	2.455506857
DIAPH1	diaphanous related formin 1(DIAPH1)	DIAPH1	0.01277735	2.483589533
STK3	serine/threonine kinase 3(STK3)	STK3	0.01527802	2.485226568
MAN2A1	mannosidase alpha class 2A member 1(MAN2A1)	MAN2A1	0.02032246	2.491580881
CYRIB	family with sequence similarity 49 member B(FAM49B)	CYRIB	0.04913288	2.492225579
SORT1	sortilin 1(SORT1)	SORT1	0.02942598	2.496640382
SLC35F6	solute carrier family 35 member F6(SLC35F6)	SLC35F6	0.00268841	2.540644189
RCN1	reticulocalbin 1(RCN1)	RCN1	0.04602544	2.543810145
MCTS1	MCTS1, re-initiation and release factor(MCTS1)	MCTS1	0.00593080	2.593394863
RAB35	RAB35, member RAS oncogene family(RAB35)	RAB35	0.00552876	2.598962734

Be continued

TXNDC5	thioredoxin domain containing 5(TXNDC5)	TXNDC5	0.00940224	2.613491011
GGCT	gamma-glutamylcyclotransferase(GGCT)	GGCT	0.00135840	2.647049962
GEMIN5	gem nuclear organelle associated protein 5(GEMIN5)	GEMIN5	0.01480464	2.654477167
BAG3	BCL2 associated athanogene 3(BAG3)	BAG3	0.03452367	2.65757298
ATP2B1	ATPase plasma membrane Ca2+ transporting 1(ATP2B1)	ATP2B1	0.00327735	2.669126958
MAMDC2	MAM domain containing 2(MAMDC2)	MAMDC2	0.02793608	2.684082243
CA4	carbonic anhydrase 4(CA4)	CA4	0.01947327	2.685525522
CCDC6	coiled-coil domain containing 6(CCDC6)	CCDC6	0.03031260	2.687741777
NOP58	NOP58 ribonucleoprotein(NOP58)	NOP58	0.00161103	2.713353466
ADGRE5	adhesion G protein-coupled receptor E5(ADGRE5)	ADGRE5	0.04433741	2.731829865
WARS2	tryptophanyl tRNA synthetase 2, mitochondrial(WARS2)	WARS2	0.03396593	2.737298269
IGFBP7	insulin like growth factor binding protein 7(IGFBP7)	IGFBP7	0.00065796	2.737729991
PLPBP	proline synthetase cotranscribed homolog (bacterial)(PROSC)	PLPBP	0.03264033	2.749460594
IAH1	isoamyl acetate-hydrolyzing esterase 1 homolog(IAH1)	IAH1	0.00740151	2.752799557
RRAGB	Ras related GTP binding B(RRAGB)	RRAGB	0.01741720	2.753260926
RRAGA	Ras related GTP binding A(RRAGA)	RRAGA	0.01741720	2.753260926
NECTIN2	nectin cell adhesion molecule 2(NECTIN2)	NECTIN2	0.04085362	2.762422824
USP47	ubiquitin specific peptidase 47(USP47)	USP47	0.01340378	2.816507645
HLA-DQB1	major histocompatibility complex, class II, DQ beta 1(HLA-DQB1)	HLA-DQB1	0.00074981	2.828034836
SGPL1	sphingosine-1-phosphate lyase 1(SGPL1)	SGPL1	0.04284258	2.836826127
TMSB10	thymosin beta 10(TMSB10)	TMSB10	0.02396017	2.841624317
DDX58	DExD/H-box helicase 58(DDX58)	DDX58	0.03525258	2.864432697
PTGES3	prostaglandin E synthase 3(PTGES3)	PTGES3	0.00022467	2.883425258
LSP1	lymphocyte-specific protein 1(LSP1)	LSP1	0.00897652	2.899681429
PTPN6	protein tyrosine phosphatase, non-receptor type 6(PTPN6)	PTPN6	0.01118396	2.912782062
IGF2R	insulin like growth factor 2 receptor(IGF2R)	IGF2R	0.02533684	2.917016517
MYADM	myeloid associated differentiation marker(MYADM)	MYADM	0.01647572	2.925858479
SDF4	stromal cell derived factor 4(SDF4)	SDF4	0.02785344	2.960812708
SBSPON	somatomedin B and thrombospondin type 1 domain containing(SBSPON)	SBSPON	0.04679579	2.964318931
NHLRC2	NHL repeat containing 2(NHLRC2)	NHLRC2	0.00783092	2.966700666
VCAM1	vascular cell adhesion molecule 1(VCAM1)	VCAM1	0.02554074	2.970817655
TRIP10	thyroid hormone receptor interactor 10(TRIP10)	TRIP10	0.03177997	2.982524829

Be continued

RRAGC	Ras related GTP binding C(RRAGC)	RRAGC	0.01939810	2.987226547
RRAGD	Ras related GTP binding D(RRAGD)	RRAGD	0.01939810	2.987226547
CFI	complement factor I(CFI)	CFI	0.03732764	3.000368147
FKBP11	FK506 binding protein 11(FKBP11)	FKBP11	0.04483646	3.018458537
SERPING1	serpin family G member 1(SERPING1)	SERPING1	0.03380180	3.034320019
MYBBP1A	MYB binding protein 1a(MYBBP1A)	MYBBP1A	0.02313738	3.105991472
ITIH4	inter-alpha-trypsin inhibitor heavy chain family member 4(ITIH4)	ITIH4	0.04232363	3.141084259
TPP2	tripeptidyl peptidase 2(TPP2)	TPP2	0.00349541	3.143233358
STX4	syntaxin 4(STX4)	STX4	0.01129320	3.152955797
ERLEC1	endoplasmic reticulum lectin 1(ERLEC1)	ERLEC1	0.00101779	3.165749748
GBA	glucosylceramidase beta(GBA)	GBA	0.00170098	3.194799966
SUPT6H	SPT6 homolog, histone chaperone(SUPT6H)	SUPT6H	0.04633251	3.248836995
PTPN1	protein tyrosine phosphatase, non-receptor type 1(PTPN1)	PTPN1	0.00993062	3.258257483
GAPVD1	GTPase activating protein and VPS9 domains 1(GAPVD1)	GAPVD1	0.01667479	3.280087674
NRP1	neuropilin 1(NRP1)	NRP1	0.02871458	3.281176757
C7	complement C7(C7)	C7	0.03770100	3.295897988
RER1	retention in endoplasmic reticulum sorting receptor 1(RER1)	RER1	0.00693527	3.415473071
GALC	galactosylceramidase(GALC)	GALC	0.00418345	3.470109987
NCOR1	nuclear receptor corepressor 1(NCOR1)	NCOR1	0.04428310	3.531877781
ABHD6	abhydrolase domain containing 6(ABHD6)	ABHD6	0.04468987	3.640876608
CYP3A5	cytochrome P450 family 3 subfamily A member 5(CYP3A5)	CYP3A5	0.00092985	3.653480429
LRCH4	leucine rich repeats and calponin homology domain containing 4(LRCH4)	LRCH4	0.00938805	3.655330055
STRA6	stimulated by retinoic acid 6(STRA6)	STRA6	0.02651764	3.70156853
LCMT1	leucine carboxyl methyltransferase 1(LCMT1)	LCMT1	0.01499566	3.707627822
UGT3A1	UDP glycosyltransferase family 3 member A1(UGT3A1)	UGT3A1	0.00226652	3.725075756
FABP5	fatty acid binding protein 5(FABP5)	FABP5	0.01752354	3.731182003
DPYSL4	dihydropyrimidinase like 4(DPYSL4)	DPYSL4	0.00438720	3.842024431
ORM2	orosomucoid 2(ORM2)	ORM2	0.03577612	3.87593157
TIAL1	TIA1 cytotoxic granule associated RNA binding protein like 1(TIAL1)	TIAL1	0.01594049	3.890716772
TIA1	TIA1 cytotoxic granule associated RNA binding protein(TIA1)	TIA1	0.01594049	3.890716772
F13A1	coagulation factor XIII A chain(F13A1)	F13A1	0.01334489	4.028664453
GAL3ST1	galactose-3-O-sulfotransferase 1(GAL3ST1)	GAL3ST1	0.00137083	4.119686971

Be continued

SNX6	sorting nexin 6(SNX6)	SNX6	0.04858406	4.135061868
EFL1	elongation factor like GTPase 1(EFL1)	EFL1	0.01399134	4.286568718
MYL1	myosin light chain 1(MYL1)	MYL1	0.02575562	4.298035993
TBC1D1	TBC1 domain family member 1(TBC1D1)	TBC1D1	0.02841964	4.331467192
PPP6C	protein phosphatase 6 catalytic subunit(PPP6C)	PPP6C	0.03538087	4.343703335
CMPK2	cytidine/uridine monophosphate kinase 2(CMPK2)	CMPK2	0.03050324	4.565721038
RASAL1	RAS protein activator like 1(RASAL1)	RASAL1	0.00085441	4.93246446
ACSL4	acyl-CoA synthetase long-chain family member 4(ACSL4)	ACSL4	0.00012933	5.145342571
CD63	CD63 molecule(CD63)	CD63	0.00255891	5.318622818
STING1	transmembrane protein 173(TMEM173)	STING1	0.00590730	5.365128027
FRAS1	Fraser extracellular matrix complex subunit 1(FRAS1)	FRAS1	0.01873524	5.563668225
CTSG	cathepsin G(CTSG)	CTSG	0.02136047	5.743526963
APOC2	apolipoprotein C2(APOC2)	APOC2	0.00342199	5.927918159
TAP2	transporter 2, ATP binding cassette subfamily B member(TAP2)	TAP2	0.01614668	5.948477005
CORO2B	coronin 2B(CORO2B)	CORO2B	0.00606066	6.65787225
TIGAR	TP53 induced glycolysis regulatory phosphatase(TIGAR)	TIGAR	0.00229833	7.638439473
COL3A1	collagen type III alpha 1 chain(COL3A1)	COL3A1	0.02368313	11.29344161
PON2	paraoxonase 2(PON2)	PON2	0.00074868	12.51402878
NNMT	nicotinamide N-methyltransferase(NNMT)	NNMT	0.00048602	13.22618989
POSTN	periostin(POSTN)	POSTN	0.03623033	13.47598519
CD163	CD163 molecule(CD163)	CD163	0.00178565	13.88223144
AMY1A	amylase, alpha 1A (salivary)(AMY1A)	AMY1A	0.02587633	34.28665782
AMY2A	amylase, alpha 2A (pancreatic)(AMY2A)	AMY2A	0.02587633	34.28665782
AMY2B	amylase, alpha 2B (pancreatic)(AMY2B)	AMY2B	0.02587633	34.28665782
PLEK	pleckstrin(PLEK)	PLEK	0.00000000	inf
NEDD8	neural precursor cell expressed, developmentally down-regulated 8(NEDD8)	NEDD8	0.01445884	inf
MCRIP1	MAPK regulated corepressor interacting protein 1(MCRIP1)	MCRIP1	0.00000000	inf
SUPT5H	SPT5 homolog, DSIF elongation factor subunit(SUPT5H)	SUPT5H	0.00000000	inf
B4GAT1	beta-1,4-glucuronyltransferase 1(B4GAT1)	B4GAT1	0.00000000	inf
SELENOF	selenoprotein F(SELENOF)	SELENOF	0.00000000	inf
ATP6AP2	ATPase H+ transporting accessory protein 2(ATP6AP2)	ATP6AP2	0.00000000	inf
YIF1A	Yip1 interacting factor homolog A, membrane trafficking protein(YIF1A)	YIF1A	0.00000002	inf
STBD1	starch binding domain 1(STBD1)	STBD1	0.00000000	inf

Be continued

AGR2	anterior gradient 2, protein disulphide isomerase family member(AGR2)	AGR2	0.00020485	inf
F12	coagulation factor XII(F12)	F12	0.00000139	inf
OAS1	2'-5'-oligoadenylate synthetase 1(OAS1)	OAS1	0.00000895	inf
ANG	angiogenin(ANG)	ANG	0.00160915	inf
C2	complement C2(C2)	C2	0.00000000	inf
SNRPC	small nuclear ribonucleoprotein polypeptide C(SNRPC)	SNRPC	0.00000000	inf
RNASE3	ribonuclease A family member 3(RNASE3)	RNASE3	0.00000000	inf
CD58	CD58 molecule(CD58)	CD58	0.00000000	inf
MRC1	mannose receptor, C type 1(MRC1)	MRC1	0.00000000	inf
NFYA	nuclear transcription factor Y subunit alpha(NFYA)	NFYA	0.00000000	inf
CPOX	coproporphyrinogen oxidase(CPOX)	CPOX	0.00000000	inf
MTHFR	methylenetetrahydrofolate reductase(MTHFR)	MTHFR	0.00000000	inf
NOP2	NOP2 nucleolar protein(NOP2)	NOP2	0.00000000	inf
SERPINB8	serpin family B member 8(SERPINB8)	SERPINB8	0.00000514	inf
ROMO1	reactive oxygen species modulator 1(ROMO1)	ROMO1	0.03231230	inf
HLA-DRB3	major histocompatibility complex, class II, DR beta 3(HLA-DRB3)	HLA-DRB3	0.00000000	inf
CCZ1B	CCZ1 homolog, vacuolar protein trafficking and biogenesis associated(CCZ1)	CCZ1B	0.00000000	inf
CCZ1	CCZ1 homolog, vacuolar protein trafficking and biogenesis associated(CCZ1)	CCZ1	0.00000000	inf
ARHGAP4	Rho GTPase activating protein 4(ARHGAP4)	ARHGAP4	0.00000054	inf
XPC	XPC complex subunit, DNA damage recognition and repair factor(XPC)	XPC	0.00000000	inf
ITIH3	inter-alpha-trypsin inhibitor heavy chain 3(ITIH3)	ITIH3	0.00000000	inf
SNTA1	syntrophin alpha 1(SNTA1)	SNTA1	0.00000000	inf
PKP1	plakophilin 1(PKP1)	PKP1	0.00000000	inf
COG2	component of oligomeric golgi complex 2(COG2)	COG2	0.00000001	inf
RRS1	ribosome biogenesis regulator homolog(RRS1)	RRS1	0.00000000	inf
CYBRD1	cytochrome b reductase 1(CYBRD1)	CYBRD1	0.00003325	inf
TBCEL	tubulin folding cofactor E like(TBCEL)	TBCEL	0.00000000	inf
EXOSC6	exosome component 6(EXOSC6)	EXOSC6	0.00000012	inf
FRY	FRY microtubule binding protein(FRY)	FRY	0.00000005	inf
RALGAPA1	Ral GTPase activating protein catalytic alpha subunit 1(RALGAPA1)	RALGAPA1	0.00000000	inf

Be continued

RCSD1	RCSD domain containing 1(RCSD1)	RCSD1	0.00000000	inf
PLBD1	phospholipase B domain containing 1(PLBD1)	PLBD1	0.00000001	inf
RIPOR1	family with sequence similarity 65 member A(FAM65A)	RIPOR1	0.00000000	inf
SPATC1	spermatogenesis and centriole associated 1(SPATC1)	SPATC1	0.00000963	inf
DHX29	DExH-box helicase 29(DHX29)	DHX29	0.00000000	inf
COMMD7	COMM domain containing 7(COMMD7)	COMMD7	0.00000000	inf
NUDCD3	NudC domain containing 3(NUDCD3)	NUDCD3	0.00000000	inf
SLC39A11	solute carrier family 39 member 11(SLC39A11)	SLC39A11	0.00000000	inf
ARL6IP6	ADP ribosylation factor like GTPase 6 interacting protein 6(ARL6IP6)	ARL6IP6	0.00000000	inf
GIMAP8	GTPase, IMAP family member 8(GIMAP8)	GIMAP8	0.00000000	inf
SH3TC1	SH3 domain and tetratricopeptide repeats 1(SH3TC1)	SH3TC1	0.00000000	inf
ZC3H15	zinc finger CCCH-type containing 15(ZC3H15)	ZC3H15	0.00001642	inf
PPP1R13L	protein phosphatase 1 regulatory subunit 13 like(PPP1R13L)	PPP1R13L	0.00000000	inf
AHCTF1	AT-hook containing transcription factor 1(AHCTF1)	AHCTF1	0.00000000	inf
OVCA2	ovarian tumor suppressor candidate 2(OVCA2)	OVCA2	0.00000001	inf
ANKS1A	ankyrin repeat and sterile alpha motif domain containing 1A(ANKS1A)	ANKS1A	0.00000000	inf
VTI1A	vesicle transport through interaction with t-SNAREs 1A(VTI1A)	VTI1A	0.00000000	inf
PPP1R14B	protein phosphatase 1 regulatory inhibitor subunit 14B(PPP1R14B)	PPP1R14B	0.00000000	inf
ELMO2	engulfment and cell motility 2(ELMO2)	ELMO2	0.00000000	inf
TMEM68	transmembrane protein 68(TMEM68)	TMEM68	0.00000005	inf
SH3GL2	SH3 domain containing GRB2 like 2, endophilin A1(SH3GL2)	SH3GL2	0.00000005	inf
NUP58	nucleoporin 58(NUP58)	NUP58	0.00000000	inf
EMILIN2	elastin microfibril interfacer 2(EMILIN2)	EMILIN2	0.00000000	inf
ZDHHC5	zinc finger DHHC-type containing 5(ZDHHC5)	ZDHHC5	0.00000000	inf
CDC42EP4	CDC42 effector protein 4(CDC42EP4)	CDC42EP4	0.00000000	inf
AGO3	argonaute 3, RISC catalytic component(AGO3)	AGO3	0.00051396	inf
RETN	resistin(RETN)	RETN	0.00000000	inf
LMBRD1	LMBR1 domain containing 1(LMBRD1)	LMBRD1	0.00000038	inf

Be continued

MARCHF5	membrane associated ring-CH-type finger 5(MARCH5)	MARCHF5	0.00000663	inf
TMOD2	tropomodulin 2(TMOD2)	TMOD2	0.00717370	inf
DPM3	dolichyl-phosphate mannosyltransferase subunit 3(DPM3)	DPM3	0.00000078	inf
PISD	phosphatidylserine decarboxylase(PISD)	PISD	0.00000000	inf
ABCF2	ATP binding cassette subfamily F member 2(ABCF2)	ABCF2	0.00000000	inf
TAGLN3	transgelin 3(TAGLN3)	TAGLN3	0.00000000	inf
MBD1	methyl-CpG binding domain protein 1(MBD1)	MBD1	0.00000000	inf
TRMT6	tRNA methyltransferase 6(TRMT6)	TRMT6	0.00000001	inf
NDUFAF1	NADH:ubiquinone oxidoreductase complex assembly factor 1(NDUFAF1)	NDUFAF1	0.00000000	inf
MRPS16	mitochondrial ribosomal protein S16(MRPS16)	MRPS16	0.00000000	inf
TSSC4	tumor suppressing subtransferable candidate 4(TSSC4)	TSSC4	0.00000000	inf
FHOD1	formin homology 2 domain containing 1(FHOD1)	FHOD1	0.01818940	inf
AP1M2	adaptor related protein complex 1 mu 2 subunit(AP1M2)	AP1M2	0.00000000	inf

Supplementary Table 4. GO enrichment terms from differentially expressed proteins

TOTAL			UP			DOWN		
GO-Term	P-value	Protein_Gene	GO-Term	P-value	Protein_Gene	GO-Term	P-value	Protein_Gene
Biological process								
cellular protein localization	0.00000277	Q96ST3:SIN3A,P08962:CD63,Q5VZM2:RRAGB,Q7L523:RRAGA,Q9HB90:RRAGC,Q9NQL2:RRAGD	cellular protein localization	0.00001717	P08962:CD63,Q5VZM2:RRAGB,Q7L523:RRAGA,Q9HB90:RRAGC,Q9NQL2:RRAGD	mitochondrial translational elongation	0.00178357	P82673:MRPS35,Q13084:MRPL28,Q9BRJ2:MRPL45
mucus secretion	0.00021667	O95994:AGR2,Q9BV40:VAMP8	positive regulation of TOR signaling	0.00009639	Q5VZM2:RRAGB,Q7L523:RRAGA,Q9HB90:RRAGC,Q9NQL2:RRAGD	mitochondrial translational termination	0.00191116	P82673:MRPS35,Q13084:MRPL28,Q9BRJ2:MRPL45
positive regulation of epithelial cell apoptotic process	0.00021667	P31483:TIA1,Q99523:SORT1	positive regulation of epithelial cell apoptotic process	0.00013882	P31483:TIA1,Q99523:SORT1	glutamate secretion	0.00262166	P63027:VAMP2,Q13136:PPFIA1
positive regulation of TOR signaling	0.00022659	Q5VZM2:RRAGB,Q7L523:RRAGA,Q9HB90:RRAGC,Q9NQL2:RRAGD	mucus secretion	0.00013882	O95994:AGR2,Q9BV40:VAMP8	positive regulation of chromatin silencing	0.00293734	Q96ST3:SIN3A
platelet degranulation	0.00055982	P08567:PLEK,P08962:CD63,P19652:ORM2,Q06033:ITIH3,Q14624:ITIH4	platelet degranulation	0.00020165	P08567:PLEK,P08962:CD63,P19652:ORM2,Q06033:ITIH3,Q14624:ITIH4	negative regulation of histone H3-K27 acetylation	0.00293734	Q96ST3:SIN3A
alcohol metabolic process	0.00064368	P43353:ALDH3B1,P48448:ALDH3B2	alcohol metabolic process	0.00041322	P43353:ALDH3B1,P48448:ALDH3B2	positive regulation of calcium-dependent cell-cell adhesion	0.00293734	Q92845:KIFAP3
cellular response to amino acid stimulus	0.00119902	Q5VZM2:RRAGB,Q7L523:RRAGA,Q9HB90:RRAGC,Q9NQL2:RRAGD	cellular response to amino acid stimulus	0.00052331	Q5VZM2:RRAGB,Q7L523:RRAGA,Q9HB90:RRAGC,Q9NQL2:RRAGD	carnitine catabolic process	0.00293734	P28330:ACADL
ethanol catabolic process	0.00127482	P43353:ALDH3B1,P48448:ALDH3B2	ethanol catabolic process	0.00082002	P43353:ALDH3B1,P48448:ALDH3B2	somatic diversification of immunoglobulins	0.00293734	Q8WYA6:CTNNBL1
lipid metabolic process	0.00180203	Q6UWR7:ENPP6,O60488:ACSL4,P05090:APOD,P43353:ALDH3B1,P48448:ALDH3B2,Q01469:FABP5	acute-phase response	0.00097630	P19652:ORM2,Q14624:ITIH4,Q86VB7:CD163	cellular ketone body metabolic process	0.00293734	P55809:OXCT1

post-Golgi vesicle-mediated transport	0.00184886	P63027:VAMP2,Q12846:STX4,Q9BV40:VAMP8	macroautophagy	0.00116359	Q5VZM2:RRAGB,Q7L523:RRAGA,Q9HB90:RRAGC,Q9NQL2:RRAGD,Q9Y4P1:ATG4B	response to methylglyoxal	0.00293734	Q96ST3:SIN3A
molecular_function								
GTPase activating protein binding	0.00127482	Q14C86:GAPVD1,Q8IVF7:FMNL3	GTPase activating protein binding	0.000820018	Q14C86:GAPVD1,Q8IVF7:FMNL3	calcium-activated potassium channel activity	0.00098624	Q9NVV0:TMEM38B,Q9Y217:MTMR6
potassium:chloride symporter activity	0.002104035	Q9UHW9:SLC12A6,Q9UP95:SLC12A4	potassium:chloride symporter activity	0.001356069	Q9UHW9:SLC12A6,Q9UP95:SLC12A4	phosphatidylglycerophosphatase activity	0.00293734	Q8WUK0:PTPMT1
aldehyde dehydrogenase [NAD(P)+] activity	0.002104035	P43353:ALDH3B1,P48448:ALDH3B2	aldehyde dehydrogenase [NAD(P)+] activity	0.001356069	P43353:ALDH3B1,P48448:ALDH3B2	NADPH dehydrogenase (quinone) activity	0.00293734	Q8N4T8:CBR4
SNARE binding	0.003327028	P63027:VAMP2,Q12846:STX4,Q96AJ9:VTI1A,Q9BV40:VAMP8	guanyl-nucleotide exchange factor activity	0.002165464	P52735:VAV2,P86790:CCZ1B,P86791:CCZ1,P98171:ARHGAP4,Q14C86:GAPVD1	NAD(P)H dehydrogenase (quinone) activity	0.00293734	Q8N4T8:CBR4
3-chloroallyl aldehyde dehydrogenase activity	0.004333097	P43353:ALDH3B1,P48448:ALDH3B2	double-stranded RNA binding	0.002445114	O95786:DDX58,P00973:OAS1,Q9H2U1:DHX36,Q9H9G7:AGO3	glycerophosphocholine cholinephosphodiesterase activity	0.00293734	Q6UWR7:ENPP6
double-stranded RNA binding	0.005399926	O95786:DDX58,P00973:OAS1,Q9H2U1:DHX36,Q9H9G7:AGO3	3-chloroallyl aldehyde dehydrogenase activity	0.002803691	P43353:ALDH3B1,P48448:ALDH3B2	arylformamidase activity	0.00293734	Q63HM1:AFMID
guanyl-nucleotide exchange factor activity	0.005583139	P52735:VAV2,P86790:CCZ1B,P86791:CCZ1,P98171:ARHGAP4,Q14C86:GAPVD1	unfolded protein binding	0.005492218	Q15185:PTGES3,Q8IVD9:NUDCD3,Q96DZ1:ERLEC1,Q9Y375:NDUFAF1	NAD+ diphosphatase activity	0.00293734	Q9BQG2:NUDT12
protein heterodimerization activity	0.007127618	O43187:IRAK2,O00267:SUPT5H,Q6GYQ0:RALGAPA1,Q7L523:RRAGA,Q9HB90:RRAGC,Q9NQL2:RRAGD,Q9UNH7:SNX6	polysaccharide binding	0.008475863	O95210:STBD1,Q8IVN8:SBSPON	chloride channel activity	0.00554550	Q96S66:CLCC1,Q9C0H2:TTYH3
unfolded protein binding	0.011803685	Q15185:PTGES3,Q8IVD9:NUDCD3,Q96DZ1:ERLEC1,Q9Y375:NDUFAF1	single-stranded RNA binding	0.008698707	O95786:DDX58,P09234:SNRPC,Q9H9G7:AGO3	proline-tRNA ligase activity	0.00586624	Q7L3T8:PARS2
polysaccharide	0.012972626	O95210:STBD1,Q8IVN8:SB	protein	0.009104582	O00267:SUPT5H,Q6	3-oxoacyl-[acyl-	0.00586624	Q8N4T8:CBR

binding		SPON	heterodimerization activity		GYQ0:RALGAPA1, Q7L523:RRAGA,Q9HB90:RRAGC,Q9NQL2:RRAGD,Q9UNH7:SNX6	carrier-protein] reductase (NADH) activity		4
cellular_component								A8MXV4:NUDT19,P28330:ACADL,P55809:OXCT1,P82673:MRPS35,Q13084:MRPL28,Q7L3T8:PARS2,Q8WUK0:PTPMT1,Q8WW59:SPRYD4,Q969Z0:TBRG4,Q96CU9:FOXRED1,Q9BRJ2:MRPL45,Q9Y2S7:POLDIP2
Gtr1-Gtr2 GTPase complex	0.00000005	Q5VZM2:RRAGB,Q7L523:RRAGA,Q9HB90:RRAGC,Q9NQL2:RRAGD	Gtr1-Gtr2 GTPase complex	0.00000002	Q5VZM2:RRAGB,Q7L523:RRAGA,Q9HB90:RRAGC,Q9NQL2:RRAGD	mitochondrion	0.00001816	
extracellular exosome	0.00000021	O60262:GNG7,P08263:GSTA1,P63027:VAMP2,Q6UWR7:ENPP6,Q8N9N7:LRRC57,Q8NCR9:CLRN3,Q92845:KIFAP3,Q9C0H2:TTYH3,O60488:ACSL4,O75223:GGCT,O75787:ATP6AP2,O94903:PLPBP,P02655:APOC2,P05090:APOD,P08311:CTSG,P08962:CD63,P12724:RNASE3,P19256:CD58,P19652:ORM2,P19961:AMY2B,P20020:ATP2B1,P22748:CA4,P33241:LSP1,P35080:PFN2,P39059:COL15A1,P43353:ALDH3B1,P46109:CRKL,P50452:SERPINB8,P50453:SERPINB9,P54803:GALC,Q01085:TIAL1,Q01469:FABP5,Q06033:ITIH3,Q12846:STX4,Q13835:PKP1,Q14624:ITIH4,Q15185:PTGES3,Q15286:	EGO complex	0.00000009	Q5VZM2:RRAGB,Q7L523:RRAGA,Q9HB90:RRAGC,Q9NQL2:RRAGD	mitochondrial matrix	0.00118176	P28330:ACADL,P55809:OXCT1,Q7L3T8:PARS2,Q8N4T8:CBR4,Q8WVM0:TFB1M

		RAB35,Q15642:TRIP10,Q15843:NEDD8,Q16706:MAN2A1,Q2TAA2:IAH1,Q53TN4:CYBRD1,Q6ZS17:RIPOR1,Q86VX2:COMMD7,Q8IV08:PLD3,Q8N357:SLC35F6,Q8NBS9:TXNDC5,Q8WYP5:AHCTF1,Q92692:NECTIN2,Q96S97:MYADM,Q9BRK5:SDF4,Q9BV23:ABHD6,Q9BV40:VAMP8,Q9GZZ1:NAA50,Q9H2U1:DHX36,Q9HAV0:GNB4,Q9NR31:SAR1A,Q9Y2T3:GDA					
EGO complex	0.00000023	Q5VZM2:RRAGB,Q7L523:RRAGA,Q9HB90:RRAGC,Q9NQL2:RRAGD	extracellular exosome	0.00000011	O60488:ACSL4,O75223:GGCT,O75787:ATP6AP2,O94903:PLPBP,P02655:APOC2,P05090:APOD,P08311:CTSG,P08962:CD63,P12724:RNASE3,P19256:CD58,P19652:ORM2,P19961:AMY2B,P20020:ATP2B1,P22748:CA4,P33241:LSP1,P35080:PFN2,P39059:COL15A1,P43353:ALDH3B1,P46109:CRKL,P50452:SERPINB8,P50453:SERPINB9,P54803:GALC,Q01085:TIAL1,Q01469:FABP5,Q06033:ITIH3,Q12846:STX4,Q13835:PKP1,Q14624:ITIH4,Q15185:PTGES3,Q15286:RAB35,Q15642:TRIP10,Q15843:NEDD8,Q16706:MAN2A1,Q2TAA2:IAH1,Q53TN4:CYBRD1,Q6ZS17:RIPOR1,Q86VX2:COMMD7,Q8IV08:PLD3,Q8N357:SLC	oxidoreductase complex	0.00293734	Q8N4T8:CBR4

				35F6,Q8NBS9:TXND C5,Q8WYP5:AHCTF 1,Q92692:NECTIN2, Q96S97:MYADM,Q9 BRK5:SDF4,Q9BV23 :ABHD6,Q9BV40:V AMP8,Q9GZZ1:NAA 50,Q9H2U1:DHX36, Q9HAV0:GNB4,Q9N R31:SAR1A,Q9Y2T3 :GDA			
lysosomal membrane	0.00000710	P08962:CD63,P79483:HLA-DRB3,P86790:CCZ1B,P8679 1:CCZ1,Q5VZM2:RRAGB,Q 7L523:RRAGA,Q8N357:SLC 35F6,Q99523:SORT1,Q9BTU 6:PI4K2A,Q9BV40:VAMP8, Q9HAV0:GNB4,Q9NUN5:L MBRD1,Q9UP95:SLC12A4, Q9Y6Q5:AP1M2	lysosomal membrane	0.00000051	P08962:CD63,P79483 :HLA-DRB3,P86790: CCZ1B,P86791:CCZ 1,Q5VZM2:RRAGB, Q7L523:RRAGA,Q8 N357:SLC35F6,Q995 23:SORT1,Q9BTU6: PI4K2A,Q9BV40:VA MP8,Q9HAV0:GNB4 ,Q9NUN5:LMBRD1, Q9UP95:SLC12A4,Q 9Y6Q5:AP1M2	chloride channel complex	0.00371620	Q96S66:CLC C1,Q9C0H2:T TYH3
condensed nuclear chromosome	0.00011995	Q92845:KIFAP3,P18754:RC C1,Q15050:RRS1,Q9H9G7:A GO3	lysosome	0.00005322	P13284:IFI30,P54803 :GALC,Q01085:TIAL 1,Q15642:TRIP10,Q5 VZM2:RRAGB,Q6P4 A8:PLBD1,Q7L523: RRAGA,Q9HB90:RR AGC,Q9NQL2:RRA GD O60488:ACSL4,O753 76:NCOR1,O76021:R SL1D1,O95210:STB D1,P08567:PLEK,P1 9256:CD58,P20020:A TP2B1,P22748:CA4, P33241:LSP1,P40222 :TXLNA,P50453:SE RPINB9,P79483:HL A-DRB3,Q12846:ST X4,Q14C86:GAPVD 1,Q16706:MAN2A1, Q7Z304:MAMDC2,Q	mitochondrial nucleoid	0.00471984	Q8WVM0:TF B1M,Q9Y2S7 :POLDIP2
lysosome	0.00028640	P13284:IFI30,P54803:GALC, Q01085:TIAL1,Q15642:TRIP 10,Q5VZM2:RRAGB,Q6P4A 8:PLBD1,Q7L523:RRAGA,Q 9HB90:RRAGC,Q9NQL2:RR AGD	membrane	0.00006313		mitochondrial inner membrane	0.00511300	P82673:MRPS 35,Q13084:M RPL28,Q8WU K0:PTPMT1, Q96CU9:FOX RED1,Q9BRJ 2:MRPL45

					8N1S5:SLC39A11,Q8TB61:SLC35B2,Q8TEQ6:GEMIN5,Q8WVV9:HNRNPLL,Q96JJ3:ELMO2,Q99999:GAL3ST1,Q9BRK5:SDF4,Q9BTU6:PI4K2A,Q9BV40:VAMP8,Q9C0B5:ZDHHC5,Q9H9G7:AGO3,Q9HD20:ATP13A1,Q9NUN5:LMBRD1,Q9NYL4:FKBP11,Q9P2X0:DPM3,Q9UP95:SLC12A4,Q9UQ03:CORO2B,Q9Y2X3:NOP58,Q9Y613:FHOD1			
membrane	0.00031198	P63027:VAMP2,Q8N9N7:LRRC57,Q8WYA6:CTNNBL1,Q96S66:CLCC1,O60488:ACSL4,O75376:NCOR1,O76021:RSL1D1,O95210:STBD1,P08567:PLEK,P19256:CD58,P20020:ATP2B1,P22748:CA4,P33241:LSP1,P40222:TXLNA,P50453:SERPINB9,P79483:HLA-DRB3,Q12846:STX4,Q14C86:GAPVD1,Q16706:MAN2A1,Q7Z304:MAMDC2,Q8N1S5:SLC39A11,Q8TB61:SLC35B2,Q8TEQ6:GEMIN5,Q8WVV9:HNRNPLL,Q96JJ3:ELMO2,Q99999:GAL3ST1,Q9BRK5:SDF4,Q9BTU6:PI4K2A,Q9BV40:VAMP8,Q9C0B5:ZDHHC5,Q9H9G7:AGO3,Q9HD20:ATP13A1,Q9NUN5:LMBRD1,Q9NYL4:FKBP11,Q9P2X0:DPM3,Q9UP95:SLC12A4,Q9UQ03:CORO2B,Q9Y2X3:NOP58,Q9Y613:FHOD1	condensed nuclear chromosome	0.00116143	P18754:RCC1,Q15050:RRS1,Q9H9G7:AGO3	peroxisomal matrix	0.00613005	A8MXV4:NUDT19,Q9BQG2:NUDT12
intracellular membrane-bounded organelle	0.00115326	P63027:VAMP2,Q96S66:CLCC1,O95070:YIF1A,P13284:IFI30,P20020:ATP2B1,P86790	intracellular membrane-bounded organelle	0.00119017	O95070:YIF1A,P13284:IFI30,P20020:ATP2B1,P86790:CCZ1B,	intraciliary transport particle	0.00878672	Q92845:KIFAP3

		:CCZ1B,P86791:CCZ1,Q138 35:PKP1,Q15642:TRIP10,Q5 VZM2:RRAGB,Q7L523:RR AGA,Q86VX2:COMMD7,Q9 HB90:RRAGC,Q9HD20:ATP 13A1,Q9Y6Q5:AP1M2			P86791:CCZ1,Q1383 5:PKP1,Q15642:TRIP 10,Q5VZM2:RRAGB ,Q7L523:RRAGA,Q8 6VX2:COMMD7,Q9 HB90:RRAGC,Q9HD 20:ATP13A1,Q9Y6Q 5:AP1M2			
mitochondrion	0.00134037	A8MXV4:NUDT19,P28330: ACADL,P55809:OXCT1,P82 673:MRPS35,Q13084:MRPL 28,Q7L3T8:PARS2,Q8WUK0 :PTPMT1,Q8WW59:SPRYD4 ,Q969Z0:TBRG4,Q96CU9:F OXRED1,Q9BRJ2:MRPL45, Q9Y2S7:POLDIP2,O94903:P LPBP,O95994:AGR2,P00973: OAS1,P36551:CPOX,P54803: GALC,P60602:ROMO1,Q152 86:RAB35,Q5EBM0:CMPK2, Q7Z478:DHX29,Q8N357:SL C35F6,Q8ND71:GIMAP8,Q8 NE86:MCU,Q9BTU6:PI4K2 A,Q9BV23:ABHD6,Q9Y3D3 :MRPS16	clathrin-coated endocytic vesicle	0.00280369	Q15286:RAB35,Q9N UN5:LMBRD1	kinesin II complex	0.00878672	Q92845:KIFA P3
secretory granule membrane	0.00257797	P63027:VAMP2,P22748:CA4, Q9BV40:VAMP8	platelet dense granule lumen	0.00473212	Q06033:ITIH3,Q1462 4:ITIH4	periciliary membrane compartment	0.00878672	Q92845:KIFA P3

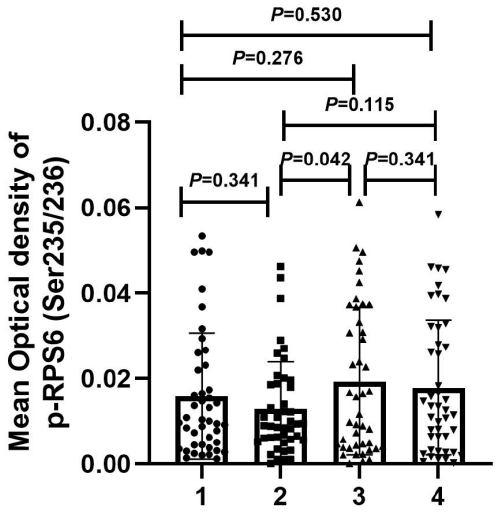

Supplementary Figure 1 The association of mTORC1 activation in glomerular area with FPW. The expression of p-RPS6 (ser235/236) in kidneys of LN patients with different quartiles of FPW. 1, 0 - 1/4; 2, 1/4 - 2/4; 3, 2/4 - 3/4; 4, 3/4 - 1. 1/4, FPW = 1107.7nm; 2/4, FPW = 1488.6nm; 3/4, FPW = 2190.5nm. FPW: foot process width.

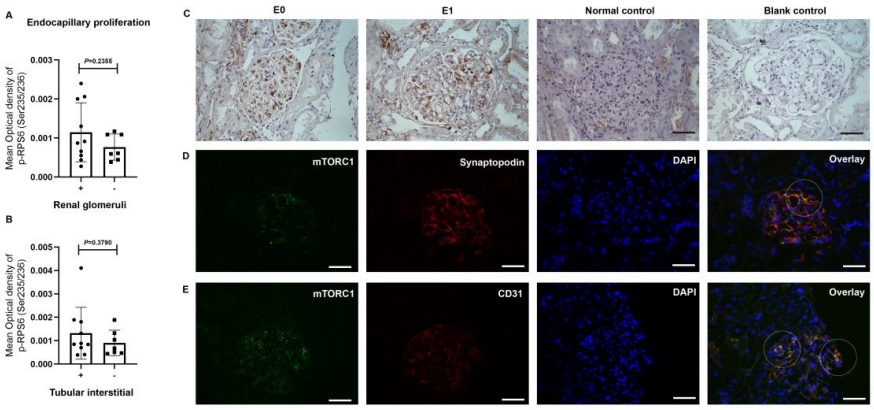

Supplementary Figure 2 The expression of p-RPS6 (ser235/236) in kidneys of IgAN patients. The mean optical density of p-RPS6 (ser235/236) (A-B) and Immunohistochemical staining of p-RPS6 (ser235/236) (C) in the glomeruli and tubulo-interstitium between IgAN with endothelial proliferation and without endothelial proliferation group respectively. (D-E) Colocalization of p-RPS6 (ser235/236) (green) and synaptopodin (green) (marker of podocyte), CD31 (red) (marker of endothelial cells). DAPI, 4′,6-diamidino-2-phenylindole (blue) (marker of nucleus). E: endothelial proliferation. Scale bar: 50 μm.

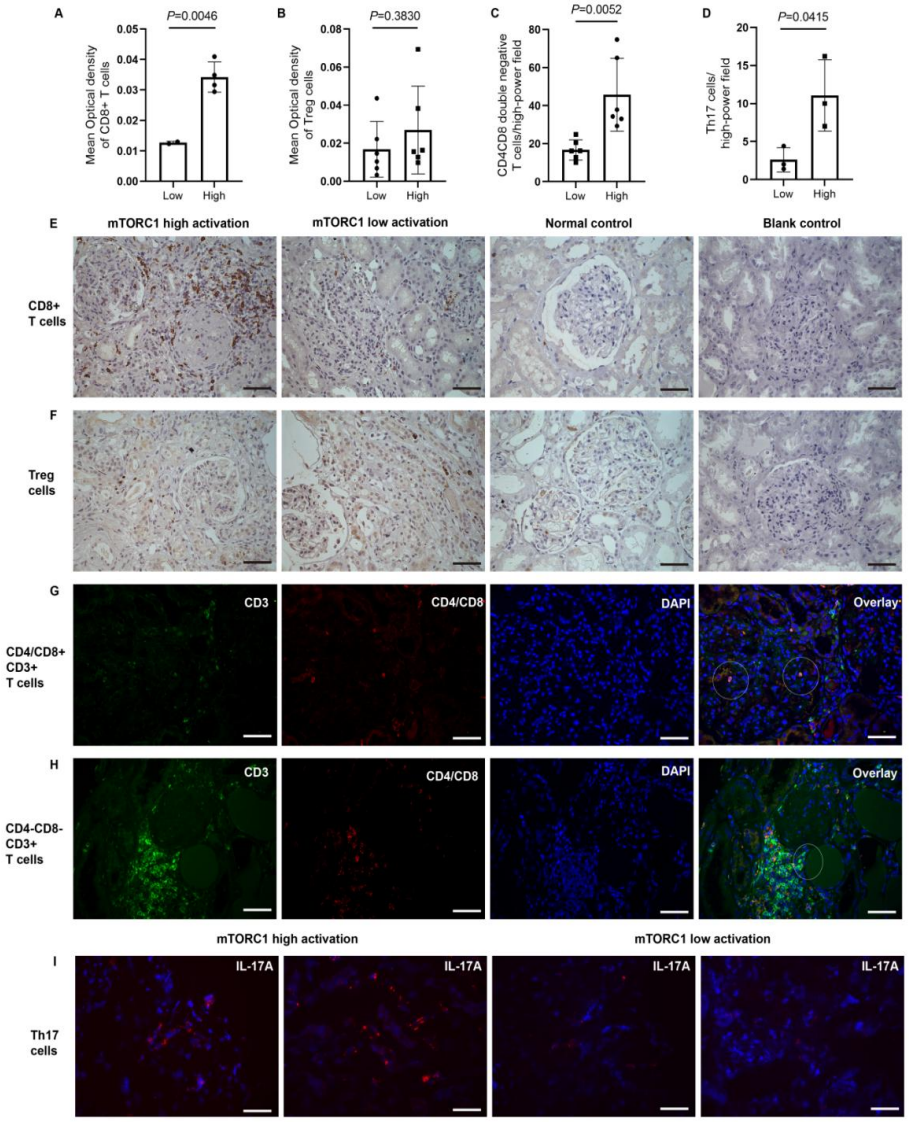

Supplementary Figure 3 The T-cell subset distribution in renal biopsies in LN patinets between mTORC1 high and low activation groups. The mean optical density of CD8+ T cells (A and E) and Treg cells (B and F) in the glomeruli and tubulointerstitium between mTORC1 high and low activation groups, respectively. The number of CD4CD8 double negative T cells (C and G-H, 200×) and Th17 cells

(D and I, 400×) per high power field. Scale bar: 50 μm.